

Litho- and Biostratigraphy of the East Mesa in Shara Murun Region of the Erlian Basin, Inner Mongolia, China, and the subdivision of the Ulangochuian Asian Land Mammal Age

Authors: Bai, Bin, Li, Qian, Zhou, Xin-Ying, Wang, Xiao-Yang, Xu, Ran-Cheng, et al.

Source: American Museum Novitates, 2025(4034) : 1-32

Published By: American Museum of Natural History

URL: <https://doi.org/10.1206/4034.1>

The BioOne Digital Library (<https://bioone.org/>) provides worldwide distribution for more than 580 journals and eBooks from BioOne's community of over 150 nonprofit societies, research institutions, and university presses in the biological, ecological, and environmental sciences. The BioOne Digital Library encompasses the flagship aggregation BioOne Complete (<https://bioone.org/subscribe>), the BioOne Complete Archive (<https://bioone.org/archive>), and the BioOne eBooks program offerings ESA eBook Collection (<https://bioone.org/esa-ebooks>) and CSIRO Publishing BioSelect Collection (<https://bioone.org/csiro-ebooks>).

Your use of this PDF, the BioOne Digital Library, and all posted and associated content indicates your acceptance of BioOne's Terms of Use, available at www.bioone.org/terms-of-use.

Usage of BioOne Digital Library content is strictly limited to personal, educational, and non-commercial use. Commercial inquiries or rights and permissions requests should be directed to the individual publisher as copyright holder.

BioOne is an innovative nonprofit that sees sustainable scholarly publishing as an inherently collaborative enterprise connecting authors, nonprofit publishers, academic institutions, research libraries, and research funders in the common goal of maximizing access to critical research.

Litho- and biostratigraphy of the East Mesa in Shara Murun Region of the Erlian Basin, Inner Mongolia, China, and the subdivision of the Ulangochuian Asian Land Mammal Age

BIN BAI,¹ QIAN LI,¹ XIN-YING ZHOU,^{1, 2} XIAO-YANG WANG,^{1, 2}
RAN-CHENG XU,^{1, 3} XIN-YUE ZHANG,^{1, 2} SHUO-SHUO QUAN,^{1, 2} JIN MENG,^{1, 4, 5}
AND YUAN-QING WANG^{1, 2}

ABSTRACT

The Paleogene deposits in the Erlian Basin are nearly continuous from the upper Paleocene to the lower Oligocene, and most Eocene Asian Land Mammal Ages were proposed on the basis of the corresponding mammal faunas from different formations in the basin. However, the correlation and extension of some lithologic units are complex and controversial in this region due to the spatial variation of the terrestrial sediments and a complex research history for more than a century. In the past decades, we have clarified the definition and correlation of the late Paleocene through early middle Eocene deposits in Huheboerhe area, but those of the middle to late Eocene deposits in Shara Murun region still remain disputable. The Ulan Gochu Formation, which was initially referred to a set of red clay at the typical Ulan Gochu locality, was considered to extend for a much wider range at East Mesa, Erden Obo, and Nom Khong. Here we provide the detailed litho- and biostratigraphy at the Bayan Obo (= Twin Oboes) and Jhama Obo sections with description of new materials of

¹ Key Laboratory of Vertebrate Evolution and Human Origins of Chinese Academy of Sciences, Institute of Vertebrate Paleontology and Paleoanthropology, Chinese Academy of Sciences, Beijing.

² College of Earth and Planetary Sciences, University of Chinese Academy of Sciences, Beijing.

³ Gansu Provincial Institute of Cultural Relics and Archaeology, Lanzhou, China.

⁴ Division of Paleontology, American Museum of Natural History, New York.

⁵ Earth and Environmental Sciences, Graduate Center, City University of New York, New York.

Eomoropus major and *Brachyhyops neimengolensis*. Deposits exposed at the Bayan Obo section can be subdivided into the Tukhum, Shara Murun, Ulan Gochu, and Baron Sog formations, totally about 70 m in thickness. The exposed strata at the Jhama Obo section can be subdivided into partial Shara Murun, Ulan Gochu, and Baron Sog formations, about 50 m in total thickness. The lithostratigraphic correlation and faunal compositions of the East Mesa are discussed based on our recent fieldworks and CAE collection records. Furthermore, the late middle Eocene Ulangochuian ALMA can be divided into Ug₁ and Ug₂, based on the mammal faunas from the upper member of the Shara Murun Formation and the Ulan Gochu Formation, respectively. The Ulangochuian is roughly correlated to the Duchesnean NALMA.

INTRODUCTION

The Erlian Basin is located in the central part of Inner Mongolia, where nearly continuous terrestrial sediments from the late Paleocene to the early Oligocene are exposed. Since the Central Asiatic Expedition (CAE) by the American Museum of Natural History in 1920s, which established the framework of the Paleogene litho- and biostratigraphy in the Erlian Basin, the Paleogene mammalian faunas from the basin have played an important role as the reference faunas in East Asia and in intercontinental correlations. More importantly, the Eocene Asian Land Mammal Ages (ALMA) are based mainly on the corresponding faunas from the Erlian Basin (Romer, 1966; Speijer et al., 2020). However, the lithostratigraphic units and their related faunas proposed by CAE need to be revised. In the past decades, we have clarified some controversies about the definitions and correlation of the late Paleocene through early middle Eocene deposits in the Huheboerhe area in the Erlian Basin (Meng et al., 2007; Sun et al., 2009; Wang et al., 2010; fig. 1), but some disputable issues are still present regarding the stratigraphy in the Shara Murun region (Radinsky, 1964a; Qiu and Wang, 2007; Wang et al., 2012; Bai et al., 2018), including the boundary between the Shara Murun and Ulan Gochu formations, and the definition of the Ulangochuian ALMA.

The Ulan Gochu Formation was named by Berkey et al. (1929) as a wedge-shaped mass of red clay along the Baron Sog Mesa. However, only *Embolotherium grangeri*, *Amyndontopsis parvidens*, and *Ardynomys olsoni* have been reported from the formation in this site (Mihlbachler, 2008; Wang and Meng, 2009; Bai et al., 2018). Most taxa previously reported as in the Ulan Gochu fauna were actually recovered from the East Mesa and Erden Obo (= Urtyn Obo), and the lumping of the assemblage is largely due to erroneous definition of the formations at Erden Obo. Recent studies restricted the Ulan Gochu Formation to the “Middle Red” beds at Erden Obo and recognized the faunal similarities and continuous deposits between the Ulan Gochu Formation and its underlying upper member of the Shara Murun Formation (Wang et al., 2012; Bai et al., 2018). Here we report the lithostratigraphy and preliminary fossil assemblage at Bayan Obo and Jhama Obo based on the fieldwork of the past several years in the East Mesa of the Shara Murun region. We further describe new material of *Eomoropus* and *Brachyhyops* from the top of the Shara Murun Formation; it is also the first report of *Eomoropus* from the Erlian Basin. More importantly, taking the advantage of detailed litho- and biostratigraphy at Bayan Obo and Jhama Obo, as well as recent fieldwork in the Shara Murun area, we propose the subdivision of the Ulangochuian ALMA.

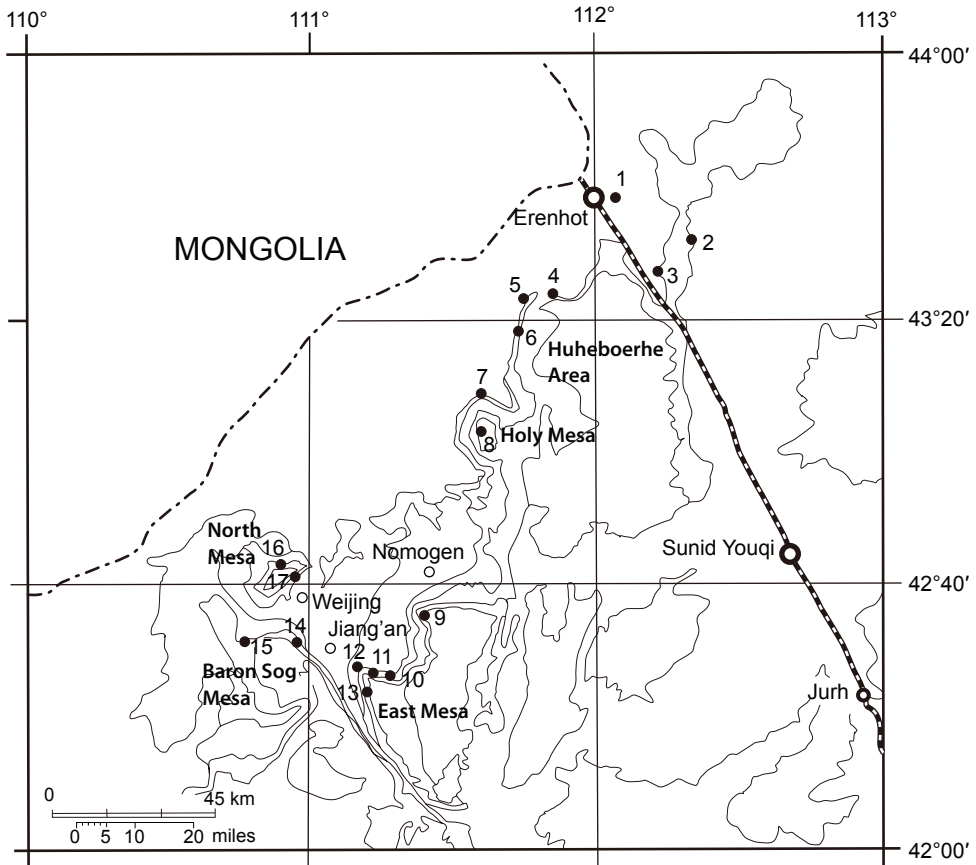


FIGURE 1. Main Paleogene fossil localities in the Erlen Basin, Inner Mongolia, China (Modified from Bai et al., 2018). 1, Houldjin. 2, Arshanto. 3, Irdin Manha. 4–6, Huheboerhe area: 4, Duheminboerhe (= Camp Margettes); 5, Nuhetingboerhe; 6, Huheboerhe. 7, Bayan Ulan. 8, Nom Khong (= Holy Mesa). 9, Erden Obo. 10–13, East Mesa: 10, Ganggan Obo (= Ulan Shireh Obo); 11, Heretu (= Spring Camp); 12, Bayan Obo (= Twin Oboes); 13, Jhama Obo. 14–15, Baron Sog Mesa: 14, Ulan Gochu; 15, Ula Usu. 16–17, North Mesa: 16, Wulanhuxiu; 17, Wulantaolegai.

INSTITUTIONAL ABBREVIATIONS: **AMNH**, American Museum of Natural History, New York; **IVPP**, Institute of Vertebrate Paleontology and Paleoanthropology, Chinese Academy of Sciences, Beijing; **MEUU**, Museum of Evolution (including former Paleontological Museum) of Uppsala University, Uppsala.

GEOLOGICAL SETTING OF BAYAN OBO (TWIN OBOES) AND
JHAMA OBO SECTIONS
A. BAYAN OBO (TWIN OBOES) SECTION

Figures 2–4

Baron Sog Formation

Endpoint coordinates (top of the section): 42°27.057' N, 111°11.814' E, 1170 m

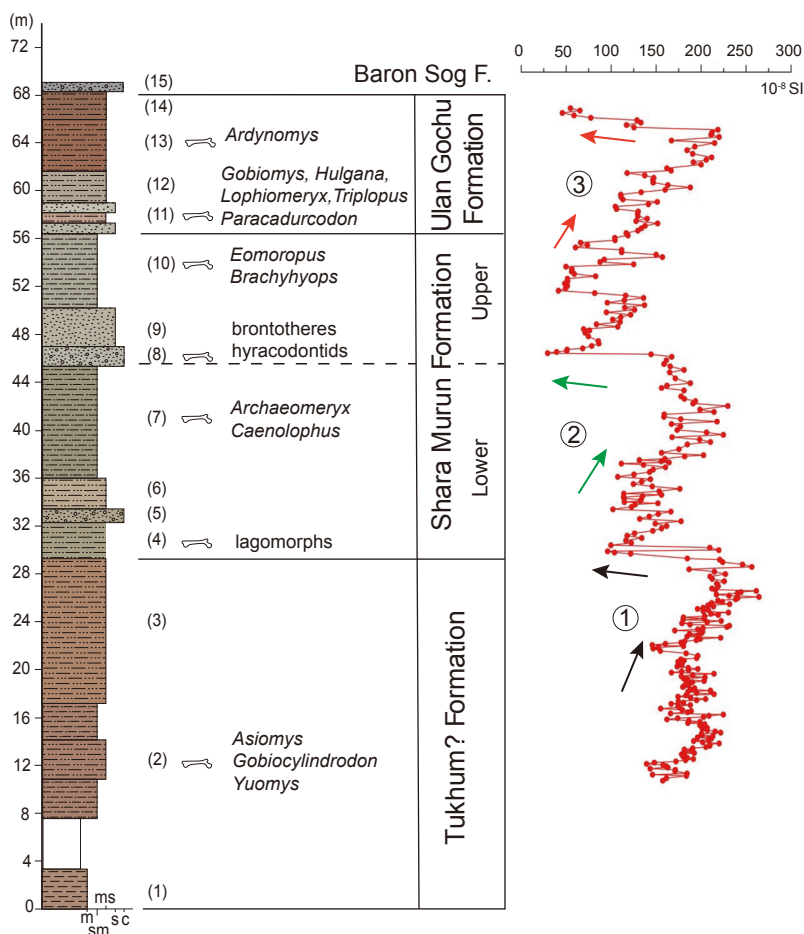


FIGURE 2. Stratigraphic column at Bayan Obo (Twin Oboes) section and magnetic susceptibility showing three cycles.

- (15) White sandy conglomerates with poorly sorted pebbles. The thickness of the bed is variable, and the maximum thickness is about 2 m. Level 68.2–69.0 m (0.8 m thick)
- Disconformity---
- Ulan Gochu Formation
- (14) Variegated muddy siltstone, containing calcareous nodules. Level 65.9–68.2 m (2.3 m thick)
- (13) Variegated (brownish red and grayish green) siltstone and silty mudstone, containing green muddy lumps at the bottom and black stains on the top. Fossils of *Ardynomys*, insectivores, and artiodactyls. Level 61.5–65.9 m (4.4 m thick)
- (12) Grayish green and brick-red silty mudstone and siltstone with muddy lumps and bedding. Level 59.3–61.5 m (2.2 m)
- (11) Light pink muddy siltstone interbedded with grayish green fine sandstone, with partly bands of red mudstones. The bottom part contains calcareous nodules. Richly fossiliferous.

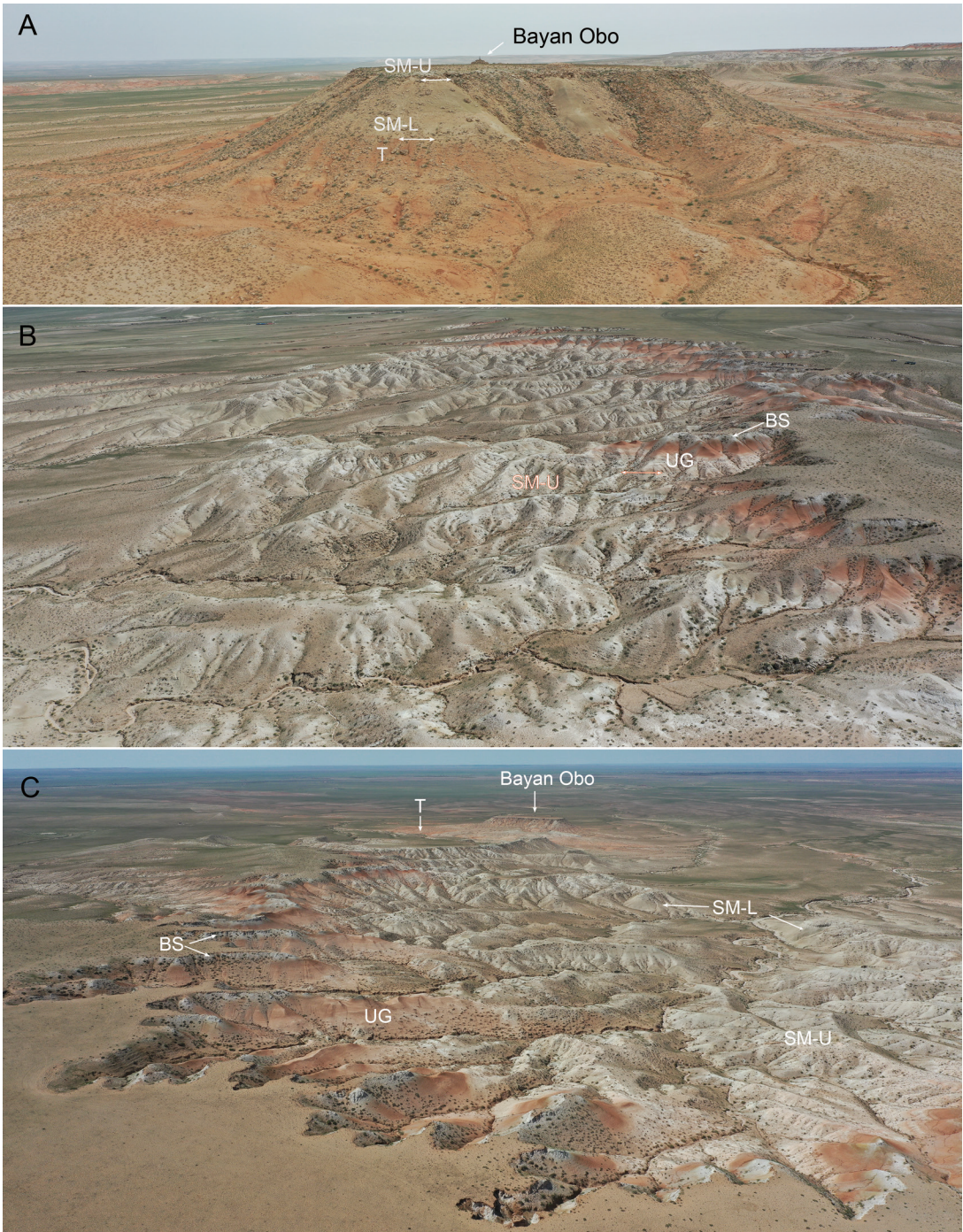


FIGURE 3. Aerial view of the Eocene outcrops at Bayan Obo section: **A**, the deposits of the Tukhum Formation (T), lower and upper members of the Shara Murun Formation (SM-L, SM-U), facing east; **B**, the deposits of the upper member of the Shara Murun Formation (SM-U), Ulan Gochu Formation (UG), and the Baron Sog Formation (BS), facing east; **C**, the deposit from bottom to the top, facing northwest.



FIGURE 4. Close view of the Eocene outcrops at Bayan Obo section: **A**, Bayan Obo (= Twin Oboes); **B**, the Tukhum Formation in the lower slope, the lower member of the Shara Murun Formation in the middle slope, and the upper member of the Shara Murun Formation on the top; **C**, the boundary between the Shara Murun and the underlying Tukhum formations as shown by arrows; **D**, **E**, the upper member of the Shara Murun Formation in the lower part, the Ulan Gochu Formation in the middle, and the Baron Sog Formation on the top. Numbers correspond to the layers of the section.

ous, including *Gobiomys*, *Hulgana*, lagomorphs, *Lophiomeryx* sp., *Paracadurcodon*, *Triplopus*, didymoconids, and lizard *Arretosaurus*. Level 56.4–59.3 m (2.9 m thick)

Shara Murun Formation

Upper Member

(10) Grayish green fine sandstone and silty mudstone. The bottom part is calciferous sandstone with 2–5 cm thick. The upper part of the beds has a lattice of calcareous nodules in some

places, where the fossils were found. Fossils of *Eomoropus major* and *Brachyhyops neimengolensis*, which are described in the present paper. Level 50.3–56.4 m. (6.1 m thick)

(9) Grayish green fine sandstone with gravels, containing calcareous nodules. Level 47–50.3 m (3.3 m thick)

(The section equivalently moved to the coordinate: 42°27.121' N, 111°11.722' E.)

(8) Thick grayish white sandy conglomerates with calcareous cementation. Fossils of brontotheres and hyracodontids. Level 45.3–47 m (1.7 m thick)

---Disconformity---

Lower Member

(7) Grayish green sandy mudstone, containing a few manganese and calcareous nodules. The upper part of the beds becomes variegated in color. Fossils of cylindrodontines, ctenodactyloids, brontotheres, *Archaeomeryx*, and *Caenolophus*. Level 36–45.3 m (9.3 m thick)

(6) Light brownish red siltstone with grayish green siltstone, with cross-bedding. Level 33–36 m (3 m thick)

(5) Grayish green sandy conglomerates, containing large amount of calcareous nodules. Level 32.1–33 m (0.9 m thick)

(4) Grayish green siltstone, with cross-bedding and black stain, and containing calcareous nodules. Fossils of lagomorphs. Level 29.1–32.1 m (3 m thick)

? Tukhum Formation

(3) Variegated (brownish red or grayish green) muddy siltstone, containing manganese nodules. The bed becomes muddier upward. Level 17.3–29.1 m (11.8 m thick)

(2) Brownish red muddy siltstone and silty mudstone, with the lower and upper parts containing calcareous and manganese nodules, and grayish green muddy lumps. Fossils of rodent *Asiomys dawsoni*, *Gobiocylindrodon* cf. *G. ulausuensis*, and *Yuomys* sp. Level 7.5–17.3 m (9.8 m thick)

Covered. Level 3.6–7.5 m (3.9 m thick)

(1) Brownish red mudstone, bearing gypsum. Level 0–3.6 m (3.6 m thick)

Starting point coordinate: 42°27.915' N, 111°10.773' E, 1094 m

B. JHAMA OBO SECTION

Figures 5–7

Baron Sog Formation

Endpoint coordinate (top of the section): 42°25.060' N, 111°12.574' E, 1199 m

(15) Rusty yellow sandy conglomerates. Level 48.0–49.1 m. (1.1 m)

(14) Grayish green, with some yellow, medium-coarse sandstone. Level 45.9–48.0 m. (2.1 m)

(13) Grayish green muddy siltstone and fine sandstone, variegated (grayish green and brickly red) medium-coarse sandstone in the bottom. Level 43.75–45.9 m. (2.15 m)

(12) Grayish green muddy siltstone with calcareous nodules. Fossils of *Ardynomys*, lagomorphs, and amynodontids. Level 41.6–43.75 m. (2.15 m)

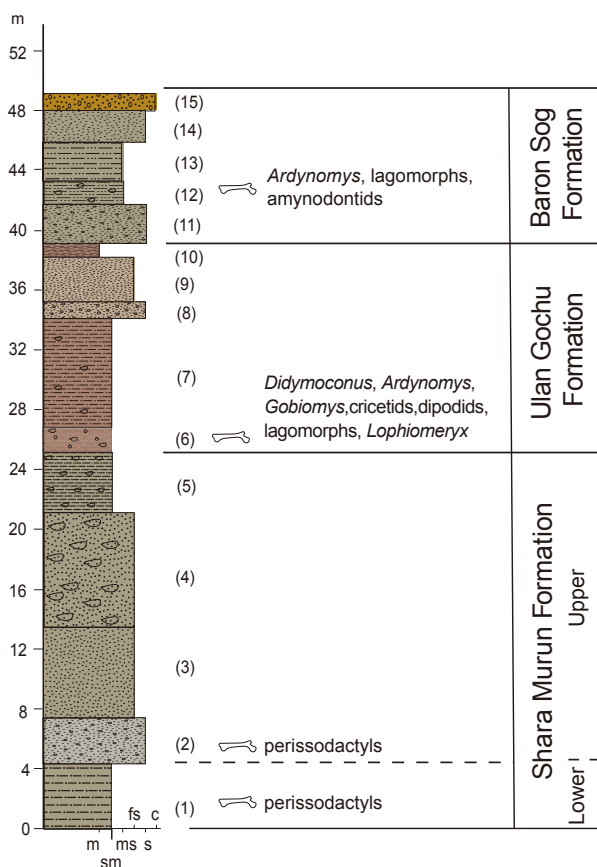


FIGURE 5. Stratigraphic column at Jhama Obo section.

(11) Grayish green pebbly coarse sandstone with locally calcareous cemented, fine sandstone on the top. Level 39.0–41.6 m. (2.6 m)

---Disconformity---

(The section equivalently moved to the coordinate: 42°25.055' N, 111°12.541' E.)

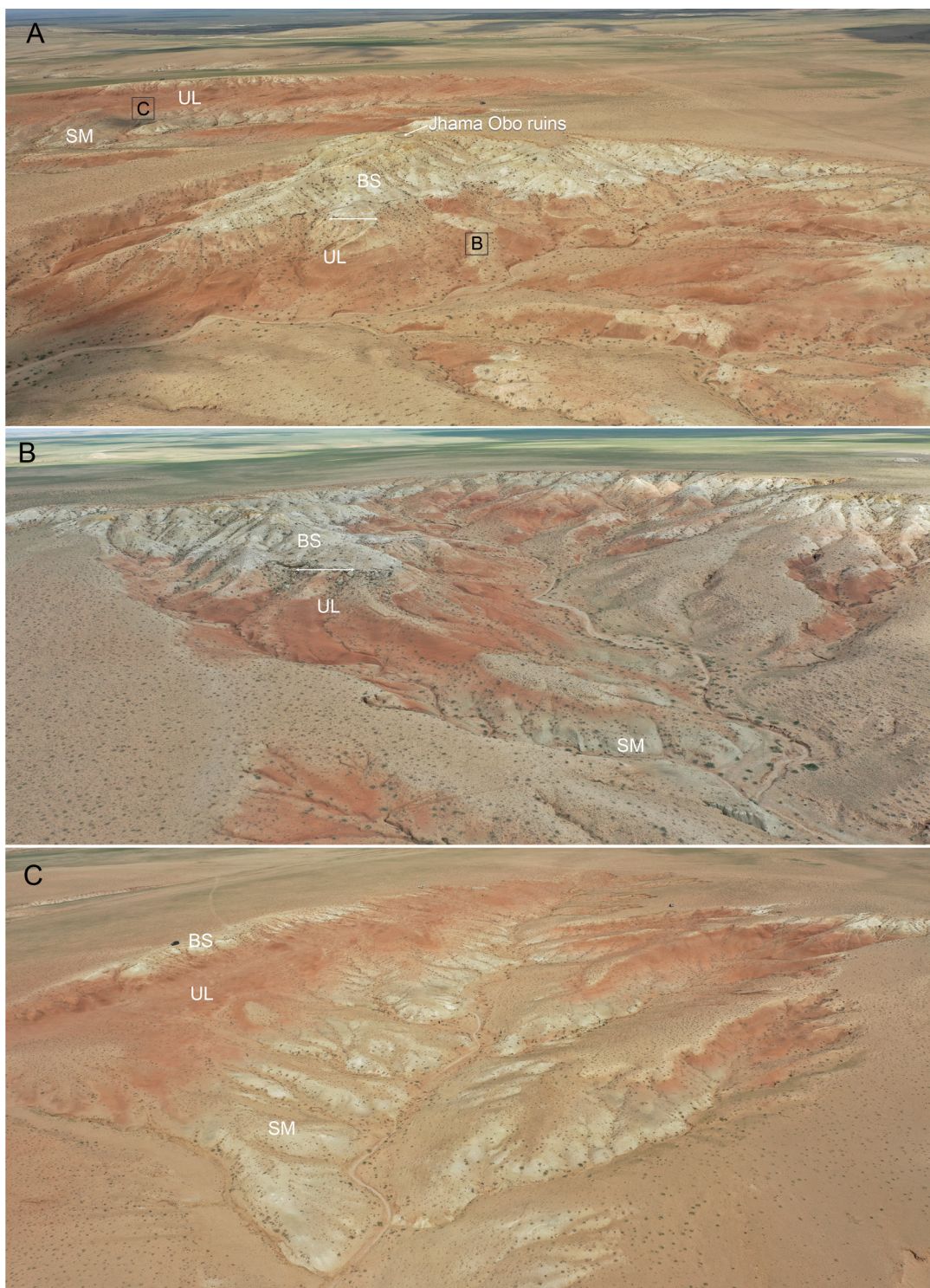
Ulan Gochu Formation

(10) Brownish red mudstone, with grayish green mudstone on the top. Fossils of lizard post-crania. Level 38.3–39.0 m. (0.7 m)

(9) Variegated (brownish red with some grayish green) muddy fine sandstone. Level 35.2–38.3 m. (3.1 m)

(8) Variegated pebbly coarse sandstone. Level 34.0–35.2 m. (1.2 m)

FIGURE 6. Eocene outcrops at Jhama Obo section with the deposits of the Shara Murun (SM), Ulan Gochu (UG), and Baron Sog (BS) formation: **A**, the outcrops mainly composed of two valleys (**B**, south of Jhama Obo; **C**, north of Jhama Obo), facing north; **B**, the valley where the section measured with a thick Baron Sog Formation, facing east; **C**, another valley with abundant small mammal fossils from the lower part of the Ulan Gochu Formation, facing east.



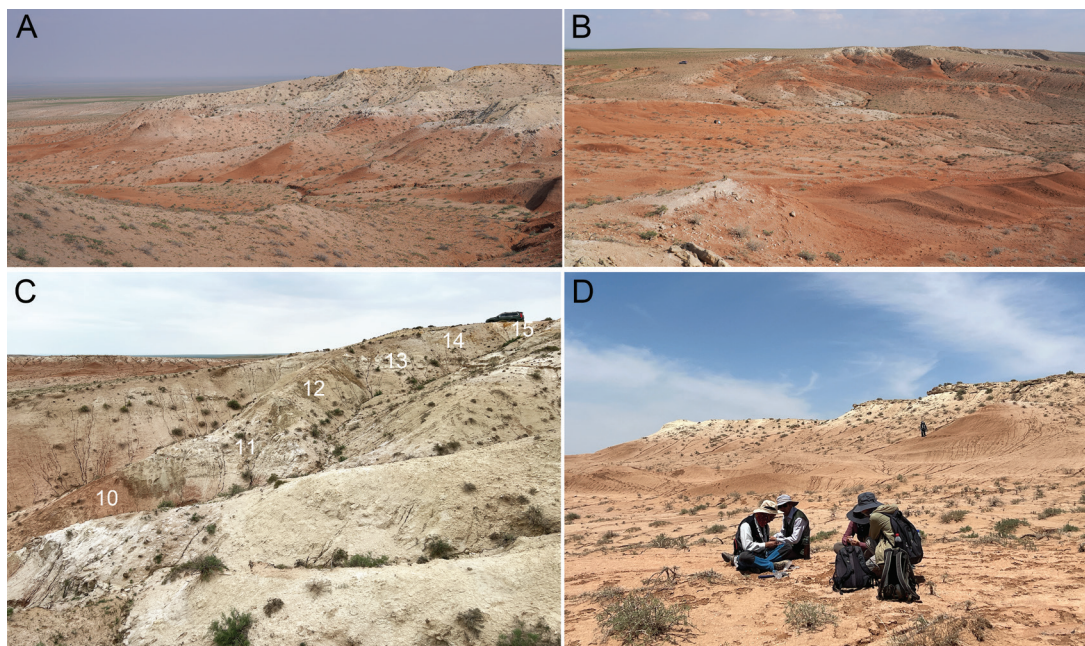


FIGURE 7. Close-up view of the Eocene outcrops at the south (A, C) and north (B, D) valleys of Jhama Obo: A–C, the red clay Ulan Gochu overlain by the gray and green sandstone/siltstone Baron Sog formations; D, collecting fossil mammals from the richly fossiliferous horizon at the base of the Ulan Gochu Formation. Numbers correspond to the layers of the section.

(7) Brownish red sandy mudstone, with a few manganese nodules and dyeing. Level 27.0–34.0 m. (7.00 m)

(6) Brownish red silty mudstone with granules, calcareous nodules, and manganese dyeing, brickly red, with some grayish green, silty mudstone in the bottom part. Abundant fossils of *Didymoconus*, *Ardynomyus*, cylindrodontids, cricetids, lagomorphs, and *Lophiomeryx*. Level 25.25–27.0 m. (1.75 m)

Shara Murun Formation

Upper Member

(5) Grayish green silty mudstone with small calcareous nodules and locally manganese dyeing, grayish green pebbly sandstone with 0.3 m thickness in the bottom part, and grayish green, with some brickly red, silty mudstone on the top. Level 21.0–25.25 m. (4.25 m)

(The section equivalently moved to the coordinate: 42°25.008' N, 111°12.400' E.)

(4) Grayish green fine sandstone and silty mudstone with large, irregularly shaped calcareous nodules, with the lower portion more sandy and upper portion more muddy and manganese dyeing. Level 13.3–21.0 m (7.7 m)

(The section equivalently moved to the coordinate: 42°25.018' N, 111°12.205' E.)

(3) Grayish green, with some yellow, fine sandstone, with gray pebbly coarse sandstone in the middle and medium-coarse sandstone above. Level 7.25–13.3 m (6.05 m)

(2) Grayish white pebbly sandstones with grayish green muddy lumps. Fossils of perissodactyl unciform and head of humerus. Level 4.2–7.25 m (3.05 m thick)

(The section equivalently moved to the coordinate: 42°25.061' N, 111°12.094' E.)

---Disconformity---

Lower Member

(1) Light grayish green muddy siltstone and silty mudstone with manganese dyeing; at the 0.5 m level, there is a lense composed of calcareous nodules with a maximum depth of ~20 cm; two thin layers of earthy yellow and variegated (earthy yellow and grayish green) muddy siltstone present at 2.7 m and 3.3 m, respectively. Fossils of perissodactyl humeral head. Level 0–4.2 m (4.2 m thick)

Starting point coordinate: 42°25.112' N, 111°11.978' E, 1150 m

SYSTEMATIC PALEONTOLOGY

Order Perissodactyla Owen, 1848

Superfamily Chalicotherioidea Gill, 1872

Family Eomoropidae Gill, 1872

Genus *Eomoropus* Osborn, 1913

Eomoropus major Zdansky, 1930

Eomoropus ? *major* Zdansky, 1930: 66, pl. 5, fig. 1-2.

Grangeria ? *major* Radinsky, 1964b: 17.

Grangeria canina Lucas and Schoch, 1989: 432, fig. 33.2H.

Eomoropus major Bai, 2008: 23.

HOLOTYPE: MEUU 3453, left M1/2.

REFERRED SPECIMEN: IVPP V 2404.1, isolated M3.

NEW MATERIAL: IVPP V 33608, probably associated right maxilla with DP2-DP4 (IVPP V 33608-1), left maxilla with DP3 (IVPP V 33608-2), and left maxilla with M2-3 (IVPP V 33608-3); IVPP V 33609, right lower jaw with m3.

LOCALITY AND HORIZON: Lok. 7, Mianchi, Henan, Rencun member of Heti Formation (MEUU 3453 and IVPP V 2404.1); Bayan Obo (= Twin Oboes), East Mesa, Siziwangqi, Inner Mongolia, Upper member of the Shara Murun Formation (IVPP V 33608–33609); middle Eocene.

EMENDED DIAGNOSIS: Differs from other species of *Eomoropus* by a larger size, metacone as large as paracone on P2, protocone of P2 somewhat anteroposteriorly extended and descending a low protoloph, and protoloph of P3 joining protocone in a low position; further differs from *E. pawnyunti* by metaloph rising to ectoloph on P3-4.

DESCRIPTION: The crown of the deciduous teeth and M2-3 are preserved in poor condition with cracks, and the permanent premolars p2-4 are in the sockets (figs. 8, 9).

DP2 is moderately worn. It is roughly triangular in outline with the width greater than the length. The ectoloph is straight, and the paracone is situated in the midline of the ectoloph with

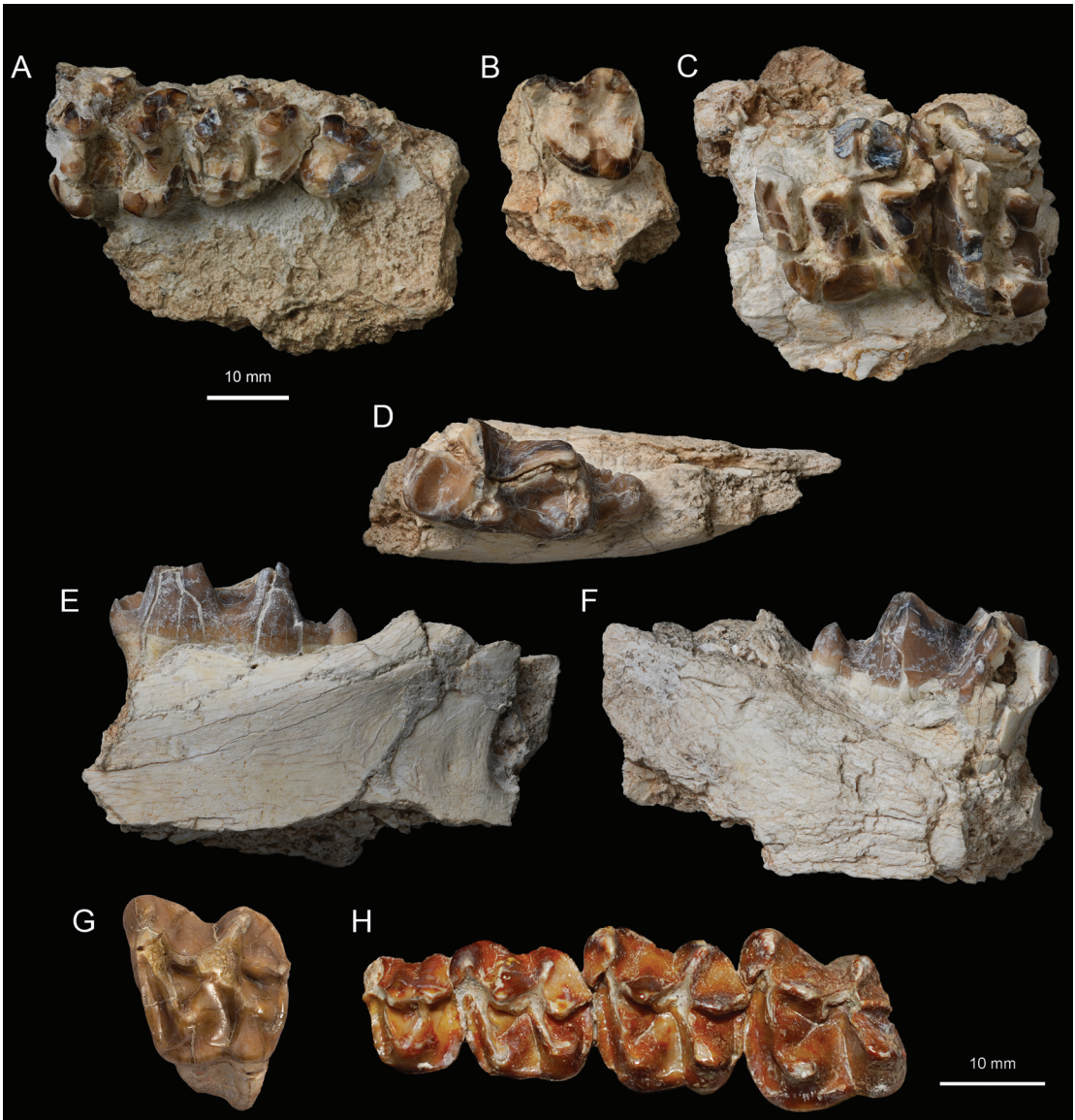


FIGURE 8. Maxillae and lower jaw of *Eomoropus major* and *E. quadridentatus*. **A–G**, *Eomoropus major*: **A**, a right maxilla with DP2–DP4 (IVPP V 33608-1); **B**, a left maxilla with DP3 (IVPP V 33608-2); **C**, a left maxilla with broken M2–3 (IVPP V 33608-3); **D–F**, a right lower jaw with m3 (IVPP V 33609); **G**, a left M1/2 (MEUU 3453); **H**, *Eomoropus quadridentatus*, a left maxilla with P4–M3 (MEUU 3451). **A–D**, **G**, **H**, occlusal view; **E**, lingual view; **F**, buccal view.

a prominent rib on the buccal side. The metacone is nearly obliterated by the heavy wear and shown by a weak buccal rib. The parastyle is partially broken, but is weak and in a low position. The protoloph, which is mainly composed of the paraconule, is shorter than and separated from the metaloph on the lingual side. The metaloph is transversely extended from the “protocone” to the metacone. A weak cingulid is present at the lingual base of the central valley.

DP3 is heavily worn. The parastyle and mesostyle are well developed with the former slightly larger. The paracone rib is relatively distinct and flatted. The protoloph is shorter and more oblique than the metaloph, and they are separated by a narrow central valley on the lingual side. The hypocone is larger than and slightly more lingually placed than the protocone. Weak anterior and posterior cingula are present. Although the crown of DP4 is cracked, it is molariform and probably square in outline. The paracone rib is ridgelike and more distinct than that of DP3. The buccal side of the metacone is flat. A small paraconule is discernable on the protoloph. The protoloph is as long as the metaloph, and separated from the latter by a wide central valley.

The P2-4 in the socket are also incomplete and partially reconstructed by the CT scanning (fig. 9). The P2 has the metacone nearly as high as the paracone, and closely placed to the latter. The paracone and metacone ribs are absent, however, the buccal surface of the ectoloph is convex. The protocone is somewhat anteroposteriorly extended. The protoloph is weaker and lower than the metaloph, descending from the protocone toward the anterolingual base of the paracone. The metaloph is strong and rises to the tip of the metacone. A distinct crista is present on the lingual side of the paracone. A prominent anterior cingulum is preserved.

The paracone and metacone of P3 are equal in height and closely placed. The paracone rib is distinct, whereas the metacone rib is weak. The protoloph joins the junction between the parastyle and preparacrista in a high position, but contacts the protocone in a relatively low position. The metaloph is strong and rises to the top of metacone as in P2.

The metacone of P4 is slightly lower than the paracone and more separated from the latter. The parastyle is well developed. The protoloph is as distinct as the metaloph, joining the anterolingual side of the paracone that is slightly lower than the ectoloph. There is a small, swollen cusp at the buccal end of the protoloph. The metaloph rises to the ectoloph in the position slightly anterior to the top of the metacone. The anterior cingulum is more distinct than the posterior one.

The two molars on the left maxilla are considered to be M2-3 rather than M1-2 based on the fact that the preserved first molar is slightly worn instead of heavily worn as on M2, and the preserved second molar is not completely erupted with a straight paracone instead of V-shaped paracone as on M3. The M2 is roughly square in outline, and the paracone and parastyle are not preserved. The mesostyle is well developed and the paraconule is distinct. The protocone is conical and not posteriorly extended. The protoloph and metaloph are complete and parallel to each other. The cingula are distinct at anterior and posterior sides of the crown, and the buccal side of the metacone. The M3 preserves only the anterior half, and is considerably wider than M2. The paracone has a prominent rib on the buccal side. The anterior cingulum is distinct.

A fragmentary right lower jaw preserves m3. The protoconid, metaconid, and "metastylid" of m3 are broken. The trigonid is wider and shorter than the talonid. The protolophid is nearly transversely extended. The paralophid is presumably long, terminating in a low paraconid at the anterolingual corner. The cristid obliqua extends anterolingually from the hypoconid to the junction of the metaconid and "metastylid" in a high position. The hypolophid is slightly

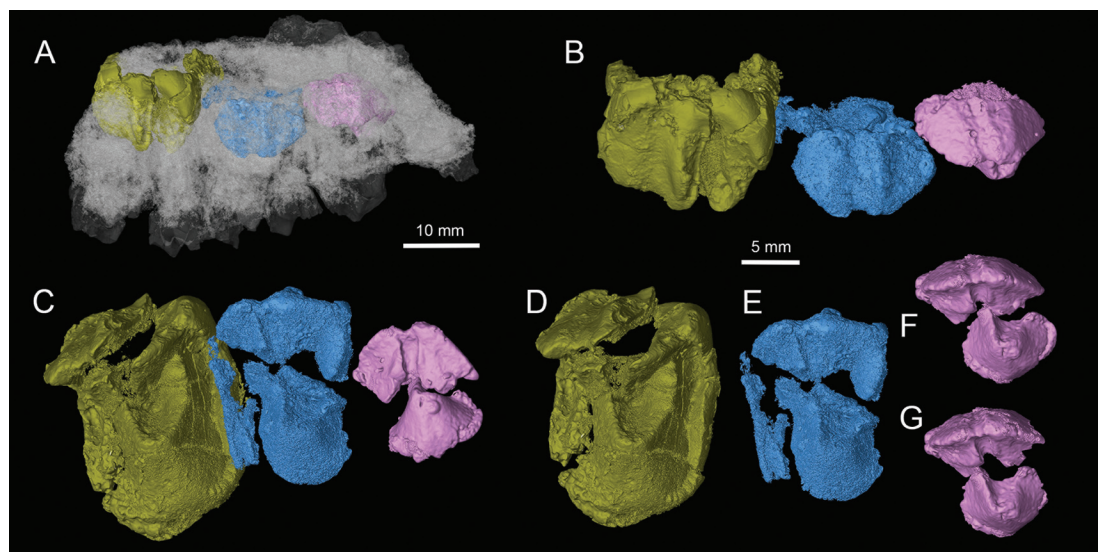


FIGURE 9. Right maxilla with DP2-4 and reconstructed P2-4 (IVPP V 33608-1) of *Eomoropus major*: **A**, P2-4 in the socket; **B–C**, right P2-4 *in situ*; **D**, right P4; **E**, right P3; **F–G**, right P2 in breakage and virtually repaired condition. **A–B**, buccal view; **C–G**, occlusal view;

oblique and probably widely notched, although the enamel is partially broken. The hypoconulid forms the third lobe and is more or less an isolated cuspid. The cingulids are present between the bases of the talonid and hypoconulid on both lingual and buccal sides. In addition, a central cristid joins the posterior base of the hypolophid to half the height of the hypoconulid.

COMPARISONS: The new specimens are characterized by a larger size than most Eocene chalicotheres. The size of M2 (length: ~21 mm; width: ~22 mm) is consistent with that of *Eomoropus major*, which is only known by isolated M1/2 (L: 20.2 mm, W: 19.9 mm) and M3 from the Rencun Member of the Hedi Formation in Mianchi, Henan (Zdansky, 1930; Hu, 1959; Bai, 2008). Although *E. major* has been assigned to *Grangeria? major* or *Grangeria canina* (Radinsky, 1964b; Lucas and Schoch, 1989), Bai (2008) still considered *E. major* to be a valid species. Furthermore, the well-developed mesostyle on M2 in the new specimens preclude its assignment to *Grangeria* or *Litolophus*, which has a relatively weaker or even absent mesostyle on the upper molars (Colbert, 1934; Gazin, 1956; Bai et al., 2010). Thus, the new materials are assigned to *Eomoropus major*, and provide new morphological information for this lesser-known species.

In addition to its large size, *Eomoropus major* mainly differs from other species of *Eomoropus* and *Grangeria* in having the metacone nearly as large as the paracone on P2 with the protocone centrally placed, anteroposteriorly extended, a descending low proto-loph, and the hypoconulid of m3 more or less an isolated cuspid. Moreover, the metaloph of P3 rises to the ectoloph in *E. major* as in other species of *Eomoropus* (except *E. pwanyunti*), whereas the metaloph of P3 connects the ectoloph in a low position in *Grangeria* and *Litolophus* (Remy et al., 2005; Bai et al., 2010). On the other hand, the proto-loph of P3 contacts the protocone in a low position as in *Grangeria canina* (Zdansky, 1930; Bai

et al., 2010). The paraconule of P3-4 is almost absent in contrast to the distinct paraconule in *Litolophus gobiensis* (Zdansky, 1930; Bai et al., 2010).

The deciduous teeth of *Eomoropus* have not been reported before the present study. The deciduous upper premolars of *Schizotherium* are known from *S. priscum* and *S. turgaicum* (Coombs, 1976). The DP2-3 of *Schizotherium* are generally more molariform than those of *Eomoropus major* in having rectangular rather than triangular outlies, equally developed proto-lophs and metalophs, which are widely separated at the lingual sides, and prominent meso-style and metacone on DP2.

Order Artiodactyla Owen, 1848

Family Entelodontidae Lydekker, 1883

Genus *Brachyhyops* Colbert, 1938

Brachyhyops neimongolensis Wang and Qiu, 2002

HOLOTYPE: AMNH 99666, right maxilla with P4–M3.

REFERRED SPECIMEN: AMNH 26264, left maxilla with DP3–4 and M1 and left lower jaw with m1-2 probably from a same individual; AMNH 99670, anterior portion of right lower jaw with dc, p1, and dp2-4; AMNH 99671, anterior portion of left lower jaw with c-p2 and root of p3.

NEW MATERIAL: IVPP V 33610, right maxilla with DP3-M2.

LOCALITY AND HORIZON: Bayan Obo, East Mesa, Siziwangqi, Inner Mongolia; Upper member of the Shara Murun Formation, middle Eocene.

DESCRIPTION: The deciduous premolars and molars are closely placed without diastemata (fig. 10).

The DP3 has two buccal cusps, with the paracone being slightly larger and higher than the metacone. A well-developed preparacrista extends anteriorly, while a strong centrocrista is composed of the postparascrista and the premetacrista. The lingual lobe exhibits a distinct protocone, which is connected to the metacone by a postprotocrista.

The DP4 is a bunodont tooth with a nearly triangular outline. It has a prominent buccal paracone and metacone. The largest lingual cusp is the protocone, followed by a slightly smaller hypocone on the posterolingual cingulum. The metaconule and paraconule are slightly larger than the hypocone. The parastyle is distinct. The preparacrista extends anteriorly, stopping at the posterior base of the parastyle. Both the postparascrista and premetacrista extend posteriorly and anteriorly respectively to form a complete centrocrista. The postmetacrista extends posteriorly, stopping at the posterior base of the metacone. Between the metacone and the metaconule, there are two cristae: one premetaconule crista extends anterobuccally and connects to the metacone, while another postmetaconule crista extends posterobuccally and connects to the posterior cingulum. A low protocrista, which is composed of a preprotocrista and a preparaconule crista, connects protocone, paraconule, and paracone. The well-developed cingula surround the anterior, posterior, and buccal sides; however, the lingual cingulum is comparatively weaker than the others. The DP4 is triple rooted, having two small buccal roots and one major lingual one.

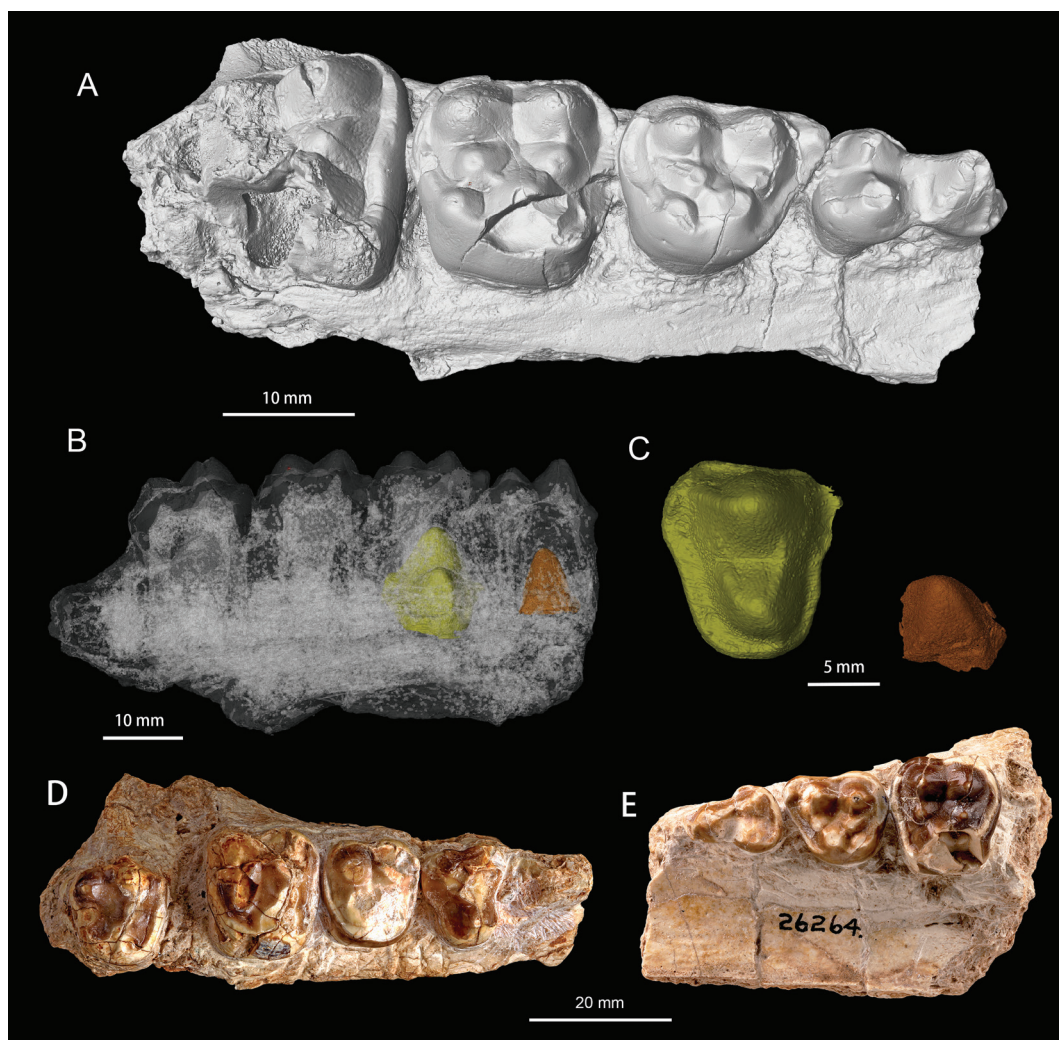


FIGURE 10. Maxillae and reconstructed P3-4 of *Brachyhyops neimongolensis*: A–C, IVPP V 33610: A, right maxilla with DP3-4, M1, and partial M2; B, right P3-4 *in situ*; C, right P3 and P4; D, a right maxilla with P4-M3 (AMNH 99666); E, a left maxilla with DP3-4 and M1 (AMNH 26264). A, C–E, occlusal view; B, lingual view. D–E modified from Zhang et al. (2023: fig. 45).

The partial P3 and P4 in the socket are reconstructed by CT scanning. P3 has only a single cone that is laterally compressed, with anterior and posterior keels, the anterior edge slightly convex and the posterior one slightly concave.

The P4 crown has two main cusps; the paracone is larger and higher than the lingual protocone. Two cristae extend from the protocone toward the buccal side, with the anterior one connecting to the paracone and the posterior one shorter, lower, and extending buccally to the lingual base of the paracone. The base of P4 is surrounded by continuous cingula and the posterior cingulum is most developed.

The trapezoidal outline of the M1 is characterized by the paracone, metacone, protocone, and hypocone, which are separated from each another by valleys. The protocone is slightly larger than the paracone, metacone, and hypocone. The paraconule is relatively smaller but distinct and is more anteriorly placed relative to the protocone and paracone. The hypocone is located posterior to the protocone and is as large as the paraconule and metaconule. The styles (parastyle, mesostyle, and metastyle) are absent in M1. The trigon basin is distinct and the cristae between the cones are weak. The weak postparacrista and premetacrista extend posteriorly and anteriorly, but the preparacrista and postmetacrista are absent. The preprotocrista and postprotocrista extend buccally from the protocone toward the paraconule and metaconule, respectively. The cingula surround the crown except at the lingual side.

The preserved portion of M2 is generally similar to the corresponding part of M1 in morphology except for its distinctly larger size.

COMPARISONS: The present new specimen from Bayan Obo shows a typical entelodontid dental morphology with six bunodont and conical upper molar cusps, bearing a distinct paraconule and metaconule. The new material has trapezoidal upper molars, cheek teeth with rather high and sharp main cusps and distinct lophs, and the protocone on M1 that is slightly larger than the hypocone. All the features are identical with those of *Brachyhyops neimongolensis*. The size of the new specimen falls within the range of variation of *Brachyhyops neimongolensis* (table 1). Wang and Qiu (2002) described *Brachyhyops neimongolensis* based on the fossils collected during the 1920s by the CAE. They described the juvenile and adult individuals of *Brachyhyops neimongolensis* from Bayan Obo. Now, the new juvenile maxilla found at the same site was micro-CT scanned, providing additional information regarding P3 and P4. In the known *Brachyhyops* species, only P3 in *B. viensis* has been reported (Storer, 1984). However, the new material from Bayan Obo indicated that the characteristics of P3 in both *B. neimongolensis* and *B. viensis* are basically similar. Both species exhibit a single major cusp in their P3, accompanied by a prominent posterobuccal ridge and a weak anterolingual ridge, but *B. viensis* is larger than *B. neimongolensis* in terms of P3 size. Compared with the upper molars in known *Brachyhyops* (*B. trofimovi*, *B. wyomingensis*, and *B. viensis*) (Colbert, 1938; Wilson, 1971; Storer, 1984; Lucas et al., 2004; Tsubamoto et al., 2011), *B. neimongolensis*, being of a relatively older age, has rather sharp main cusps and developed cristae on its cheek teeth, which are plesiomorphic characters in *Brachyhyops*.

DISCUSSION

CORRELATION OF THE BAYAN OBO AND JHAMA OBO SECTIONS

The strata at Bayan Obo can be correlated to the Tukhum and Shara Murun formation at Ula Usu, the Ulan Gochu Formation at Ula Gochu, and the Baron Sog Formation at Baron Sog (Berkey and Morris, 1927; Berkey et al., 1929; Wang et al., 2012). Layers 1–3 at Bayan Obo section are dominated by brownish red muddy siltstone, which is similar to the red clay of the Tukhum Formation or the upper part of the Ulan Shireh Formation (Li, 2024; fig. 11). In addition, layer 2 produces the rodent *Asiomys dawsoni*, *Gobiocyllindrodon*

Table 1. Measurements of teeth of *Brachyhyops neimongolensis* (mm).

	IVPP V 33610		AMNH 26264, 99666 (Wang and Qiu, 2002)	
	Length	Width	Length	Width
DP3	14.1	9.42	14.1	9.4
DP4	14.92	12.43	14.5	13.1
P3	8.01	6.58	-	-
P4	12.72	14.17	11.9	14.4
M1	15.3	16.08	13.6–15.2	15.7–16.5
M2	16.08	18.22	15.6	18.5

cf. *G. ulausuensis*, and *Yuomys* sp., which are typical fossils of the late Irдинmanhan ALMA (Li, 2024). Layers 4–7 are mainly composed of grayish-green siltstone and sandy mudstone, which are lithologically correlative to the sandy clay with varied colors of the lower member of the Shara Murun Formation at Ula Usu (Berkey and Morris, 1927; Wang et al., 2012; Li and Li, 2023). Fossil mammals of the typical Sharamurunian fauna, including *Archaeomeryx* and *Caenolophus*, have been discovered from layer 7. The boundary between the Shara Murun Formation and its underlying Tukhum Formation is continuous without notable hiatus. However, a hiatus is present between the Shara Murun Formation and its underlying Tukhum Formation at Ula Usu. Layer 8 has grayish-white sandy conglomerates, and there is a disconformity contacting the underlying layer 7. Layers 9–10 are mainly composed of grayish-green fine sandstone and silty mudstone. The chalicothere *Eomorphus major* and entelodont *Brachyhyops neimongolensis*, described above, are found from layer 10. Layers 8–10 can be correlated to the white and light-gray sandstone with gravels of the upper member of the Shara Murun Formation at Ula Usu. Layer 11 is light-pink muddy siltstone bearing abundant fossils, and layers 12–14 are dominated by variegated siltstone and mudstone. Typical Ulangochuan taxa *Lophiomeryx* and *Hulgana* have been found in layer 11. Layers 11–14 are lithologically correlated to the red clay of the Ulan Gochu Formation at Ulan Gochu. It is noteworthy that the boundary between the Ulan Gochu and Shara Murun formation is continuous. Layer 15 has white sandy conglomerates and is correlated to the Baron Sog Formation, which is characterized by the light-gray clays and fine cross-bedded sands at Baron Sog (Berkey et al., 1929). Layer 15 has a disconformity contact with the underlying Ulan Gochu Formation.

In addition, the magnetic susceptibility, which is measured by a handheld KT-10 magnetic susceptibility meter with a resolution of 10–20 cm, at the Bayan Obo section shows clear three major cycles (fig. 2), roughly corresponding to the Tukhum Formation, the lower member of the Shara Murun Formation, and the lithologic unit composed of the upper member of the Shara Murun Formation and Ulan Gochu Formation, respectively. The values of magnetic susceptibility generally increase from the bottom to the top in each cycle, then abruptly drop near the boundary of the lithologic units. The magnetic susceptibility also

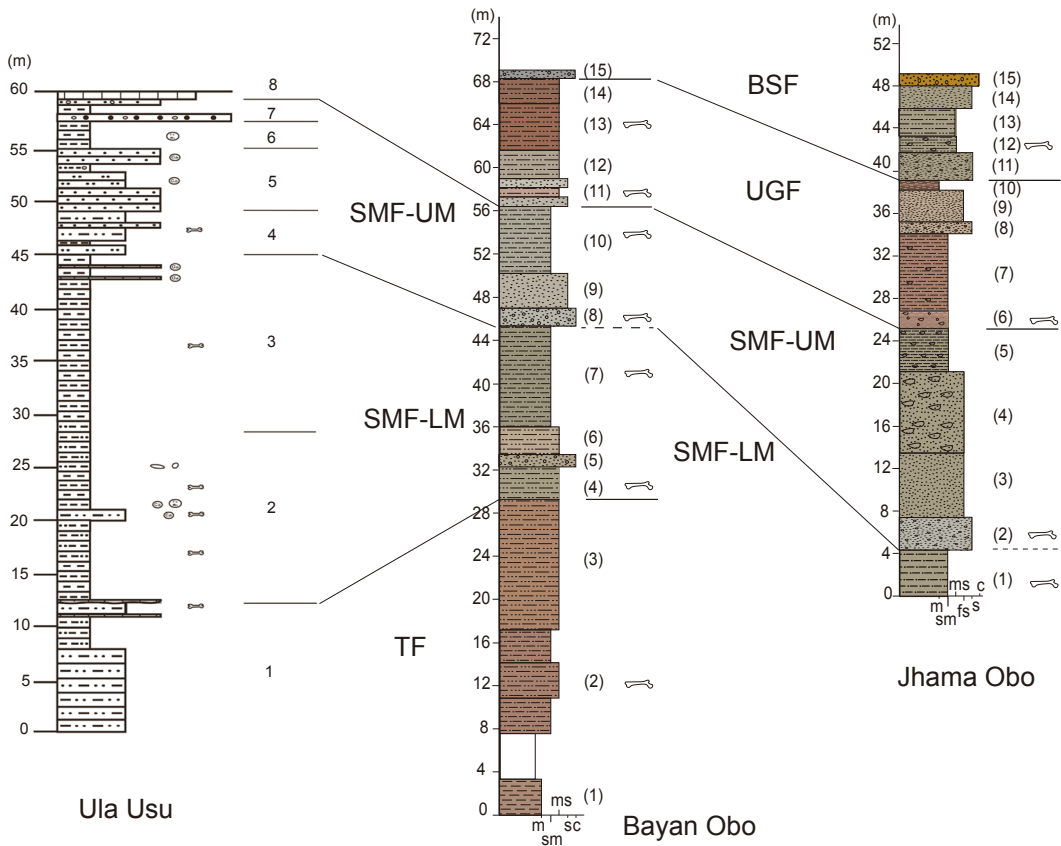


FIGURE 11. Stratigraphic correlations of the Tukhum Formation (TF), lower and upper members of the Shara Murun Formation (SMF-LM, SMF-UM), Ulan Gochu Formation (UGF), and the Baron Sog Formation (BSF) at Ula Usu (modified from Li and Li, 2023), Bayan Obo, and Jhama Obo.

suggests that the upper member of the Shara Murun Formation and the Ulan Gochu Formation need to be combined into a lithologic unit, and are separated from the underlying lower member of the Shara Murun Formation. However, the redefinition of the Ulan Gochu Formation is beyond the scope of present paper.

The section at Bayan Obo (i.e. Dahser Hai, Tasa Erhai) was sketched by Granger (1928; fig. 12). The profile is generally consistent with present section we observed at Bayan Obo. The “Baron Sog” bed is a 3.7 m (12 ft) thick conglomerate, and is equivalent to layer 15. The “Ulan Gochu” bed mainly consists of red clay with the thickness ranging from 2.1 m to 4.6 m (7–15 ft), and is probably equivalent to beds 11–14 as the Ulan Gochu Formation. However, the thickness of the Ulan Gochu Formation is 11.8 m in the present paper. The “Shara Murun” bed is composed of upper sandy-clay member 35.7 m (117 ft) in thickness, and lower conglomerates (and sandstone) 38.1 m (125 ft) in thickness. The upper and lower member of the “Shara Murun” bed are probably equivalent to layers 8–10 (11.1 m) and 4–7 (16.2 m) of the Shara Murun Formation, respectively. The basal part of the profile is “lower red,” presumably equivalent to beds 1–3 of the Tukhum Formation. Osborn

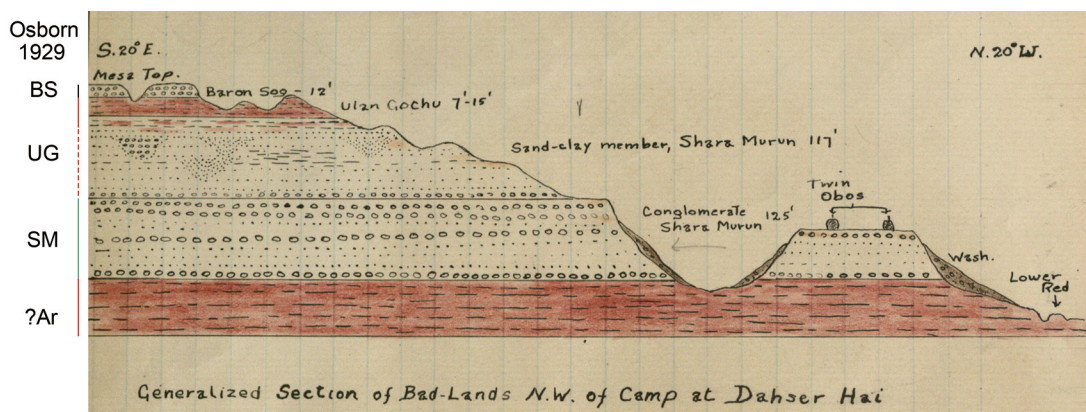


FIGURE 12. Sketch profile from Bayan Obo section by Granger (1928: 18) and the correlation proposed by Osborn (1929).

(1929) published Granger's sketch at Twin Oboes and Hospital Camp with some modifications; he considered the "sandy clay" to be "probably Ulan Gochu (upper portion at least)," and the "lower red" to be "?Arshanto" (fig. 12). However, our field investigation concurs with Granger's (1928) original interpretation of the section at Twin Oboes, which is roughly comparable to the subdivision we propose in this study.

The section at Jhama Obo can be correlated to the Bayan Obo section, but shows some variation as in the terrestrial deposits (fig. 11). The lower member of the Shara Murun Formation at Jhama Obo is mainly exposed by the top portion, and its lower portion is largely covered (layer 1). Layers 2–5 are the upper member of the Shara Murun Formation and correlated to layers 8–10 of the Bayan Obo section; the thickness of the former is about 10 m greater than that of the latter. Similarly, a notable hiatus is present between the lower and upper members of the Shara Murun Formation. Layers 6–10 of 13.75 meters in thickness at Jhama Obo are the Ulan Gochu Formation and correlated to layers 11–14 of 11.8 m in thickness of the Bayan Obo section. Similarly, the Ulan Gochu Formation is continuously deposited with the underlying Shara Murun Formation. Layers 11–15 at Jhama Obo are the Baron Sog Formation, which is about 10 m in thickness and is much thicker than in Bayan Obo. The different thickness of the Baron Sog Formation at Bayan Obo and Jhama Obo can be mainly attributed to the different erosion by the gravels of the Gobi upland.

The boundary between the Ulan Gochu Formation and the underlying Shara Murun Formation is difficult to determine due to the continuous deposits between the two formations. In a correspondence, Granger wrote to Osborn that "we have set off the 'Ulan Gochu beds' from the 'Shara Murun' on the basis of faunal change only" (Osborn, 1929: 4). Furthermore, Granger (1928: 9) noted that "the line between the two formations at Twin Oboes and Jhama Obo are not determined." Similarly, the boundary between the Ulan Gochu and Shara Murun formations at Bayan Obo and Jhama Obo is indeed partly based on the appearance of some new taxa, including *Gobiolagus andrewsi*, *Desmatolagus vetustus*, *Hulgana ertinia*, *Ardynomys olsoni*, *Embolotherium grangeri*, and probably *Lophiomeryx*.

BIOSTRATIGRAPHY OF THE EAST MESA

The specimens collected by CAE from the East Mesa are listed in appendix 1. The fossil mammals from Bayan Obo (= Twin Oboes) collected by CAE include *Brachyhyops neimongolensis*, *Lophiomeryx angarae*, *Deperetella* cf. *D. cristata*, *Juxia sharamurenensis*, *Triplopus turgaiensis*, *Metamynodon* sp., *Mongolestes hadrodens*, and *Cryptomanis gobiensis* from the Shara Murun Formation, and *Embolotherium grangeri*, *Titanodectes minor*, *Anagale gobiensis*, and *Gobiolagus andrewsi* from the Ulan Gochu Formation. Several specimens were recorded “from surface, just below Ulan Gochu” including *Gobiolagus andrewsi*, *Desmatolagus vetustus*, and *Brachyhyops neimongolensis*, and their horizons remain ambiguous as possibly rolling down from the upper strata.

The specimens from Jhama Obo and south of Jhama Obo collected by CAE are mainly from the Ulan Gochu Formation instead of initially labelled “Shara Murun Formation” as crossed by Granger in his field notes. Fossil mammals from the Ulan Gochu Formation at Jhama Obo include *Brachyhyops* sp., *Cadurcodon matthewi*, *Amynodontopsis parvidens*, *Urtinotherium intermedium*, *Embolotherium andrewsi*, *Nasamplus progressus*, *Titanodectes ingens*, *Mongolestes hadrodens*, cf. *Harpagolestes*, *Hyaenodon pervagus*, *H. sp.*, *Gobiolagus andrewsi*, *Desmatolagus vetustus*, *Hulgana ertinia*, *Ardynomyus* sp., and *Didymoconus* sp. Only two species were recorded from the Ulan Gochu Formation south of Jhama Obo: *Embolotherium andrewsi* and *Amynodontopsis tholos*. In addition, two species were discovered from or possibly from the Baron Sog Formation at Jhama Obo and south of Jhama Obo, respectively: *Urtinotherium parvum* and *Amynodontopsis parvidens*. However, there are some contradictions with previous viewpoints: two specimens of *Embolotherium andrewsi* (AMNH 26010, 26009) were recorded from the Ulan Gochu Formation from Jhama Obo and south of Jhama Obo, but the species was considered to be restricted to the overlying Baron Sog Formation and its equivalent layers (Bai et al., 2018). Specimens of *Amynodontopsis tholos* (AMNH 26031) and *A. parvidens* (AMNH 26178) were recorded from the Ulan Gochu Formation and possibly Baron Sog Formation south of Jhama Obo, respectively. However, *A. parvidens* is known from the “Lower White” and “Middle Red” beds at Erden Obo, which are correlative to the upper part of the Shara Murun Formation and Ulan Gochu Formation (Bai et al., 2018); the holotype of *Amynodontopsis tholos* was unearthed from the bed at Ulan Shireh Obo (= Ganggan Obo), which is probably correlative to the Baron Sog Formation based on our recent field work. These contradictions could be attributed either to the extension of specific distribution, or to the erroneous identifications of some specimens, or to the disputable stratigraphic correlation in the Shara Murun area.

The “Ulan Shireh Obo” locality named by CAE is actually today’s Ganggan Obo (Wang et al., 2012), which is situated about 11.4 km southeast of the Bayan Obo (about 4 miles east of Spring Camp). Three species have been recorded from the “top of gray Ulan Gochu beds,” including *Embolotherium andrewsi*, *Amynodontopsis tholos*, and *Zaisanamynodon borisovi*. *Embolotherium andrewsi* and *Zaisanamynodon borisovi* are typical taxa of the late Eocene Baron Sog Formation or equivalent beds, which are relatively well exposed at Ganggan Obo area and characterized by grayish-green mudstone and grayish-white sandstone based on our

recent field works. Similarly, the Baron Sog Formation from the Baron Sog Mesa is characterized by light-gray clays and fine cross-bedded sands with some beds containing white marly concretions (Berkey et al., 1929). Thus, the “top of gray Ulan Gochu beds” by CAE at Ulan Shireh Obo is otherwise correlated to the Baron Sog Formation. A lower jaw of *Juxia sharamurunensis* (AMNH 26036) was recorded from the “Ulan Gochu beds” at “Ulan Shireh Obo,” however, the species is a typical taxon of the Shara Murun fauna and needs further confirmation of its identification and horizon.

The “Spring Camp” of the CAE (today’s Heretu) probably derived its name from a spring that is still present in the valley of the escarpment at Heretu. The following species are documented from the Shara Murun beds at Heretu: *Tianodectes minor*, *Parabrontops* cf. *P. gobiensis* (AMNH 26131), *Pterodon hyaenoides*, *Sharamynodon mongoliensis*, *Pappaceras minuta* (AMNH 26056), *Cadurcodon ardyensis*, and amynodontids. Most species are typical taxa of the Shara Murun Formation except for *Parabrontops gobiensis* and *Pappaceras minuta* that were previously known from the “Middle White” bed at Erden Obo and the Arshanto Formation in Huheboerhe area, respectively. Further investigation is needed to clarify the residential beds of these two species. Furthermore, *Protitian grangeri* (= holotype of *P. bellus*, AMNH 26104) was recorded from the “lower red beds” at “Spring Camp,” which is probably correlative to the Irdin Manha Formation rather than the Arshanto Formation.

SUBDIVISION OF ULANGOCHUIAN ALMA

The Ulangochuian ALMA as well as some other Eocene ALMAs were established mainly based on the mammalian faunas from the Erlian Basin by Romer (1966). The age of the Ulangochuian was considered to be the early Oligocene (Li and Ting, 1983; Tong et al., 1995) or the late Eocene (Wang, 1997). Recently, based on the preliminary results of paleomagnetism, Wang et al. (2019) considered the Ulangochuian stage to be latest middle Eocene and earliest late Eocene, spanning from chron C18.2n to C17.1n, which was followed by the Paleogene Time Scale in 2020 (Speijer et al., 2020). It is necessary to mention that the age of the Ulangochuian is based on the correlation of preliminary paleomagnetic results of the “Lower White” and “Middle Red” layers at Erden Obo, which can be roughly correlated to the upper member of the Shara Murun Formation and Ulan Gochu Formation, respectively. In addition, recent analyses of perissodactyl and rodent assemblages from Ulangochuian are also mainly based on fossils from the “Lower White” and “Middle Red” layers at Erden Obo, as well as the upper member of the Shara Murun Formation and the Ulan Gochu Formation (Bai et al., 2020; Li et al., 2022). Bai et al. (2020) proposed the hypothesis of “Ulan Gochu Decline” to designate the most conspicuous decrease of perissodactyl diversity that occurred during Ulangochuian rather than at the Eocene-Oligocene transition in Asia. The rodent diversity at generic level shows a similar clear decrease during the Ulangochuian in Asia (Li et al., 2022).

Given that the Ulangochuian is actually based on mammalian faunas with somewhat different compositions from two lithological units, we suggest subdividing the Ulangochuian into two subunits: Ug₁ on the basis of the mammalian fauna from the upper member of the Shara

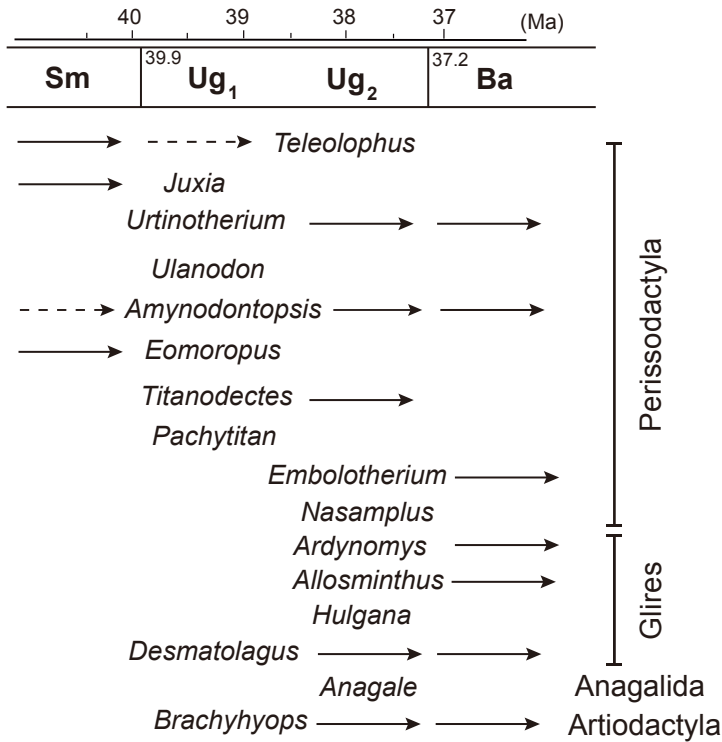


FIGURE 13. Distribution of some typical taxa in the Ulangochuian Asian Land Mammal Age. Taxa represent the first or last appearances.

Murun Formation, and Ug₂ from the Ulan Gochu Formation (fig. 13). Taxa making the first appearance in Ug₁ include *Amyndontopsis parvidens*, *Urtinotherium parvum*, *Juxia shouii*, *Ulanodon*, *Titanodectes minor*, *Pachytitan ajax*, *Desmatolagus vetustus*, *Anatolechinos neimongolensis*, and possibly *Brachyhyops neimongolensis* (Wang, 2007; 2008; Bai et al., 2018; Li, 2018; Bai and Qi, 2022). *Juxia* and *Eomoropus major* have their last appearances in Ug₁. Taxa only known from Ug₁ include *Ulanodon* and *Pachytitan ajax*.

Taxa making the first appearance in Ug₂ include *Embolotherium grangeri*, *Nasamplus progressus*, *Titanodectes ingens*, *Teleolophus magnum*, *Amyndontopsis tholos*, *Urtinotherium intermedium*, *Gobiolagus andrewsi*, *Hulgana ertinia*, *Ardynomys olsoni*, *Allosminthus gobiensis*, *A. erons*, *Anagale gobiensis*, and *Hyaenodon pervagus* (Burke, 1941; Meng et al., 2005; Bastl et al., 2014; Bai et al., 2018; Li, 2018). Taxa making the last appearance in Ug₂ include deperetellids, *Titanodectes*, *Brachyhyops neimongolensis*, and *Mongolestes hadrodens*. Taxa only known from Ug₂ include *Embolotherium grangeri*, *Nasamplus*, *Anagale gobiensis*, and *Hulgana ertinia*.

The correlations between Paleogene ALMA and NALMA are still controversial. In terms of Ulangochuian ALMA, Romer (1966) correlated the Ulangochuian to Chadronian NALMA, which was then considered being the early Oligocene. Tong et al. (1995) correlated the Ulangochuian to Orellan NALMA as the early Oligocene. Wang (1997) proposed the Ulangochuian be the part of the late Eocene that probably consisted of Naduan, Ulangochuian, and Houldjiniian in China; thus,

Ulangochuian could be partly correlated to the Chadronian NALMA. Bai et al. (2018) tentatively correlated the Ulangochuian to the Duchesnean mainly based on the *Amyndontopsis* known from both biochrons. *Amyndontopsis parvidens* from the Ulangochuian shares important similarities with *A. bodei* from Duchesnean of North America (Stock, 1933; Wall, 1981; Lucas, 1992). Wang et al. (2020) named *A. jiyuanensis*, which is Sharamuronian in age and more primitive than other species of *Amyndontopsis*, from the Niezhuang Formation of the Jiyuan Basin, Henan Province. In addition, the first appearances of *Ardynomys*, *Brachyhyops*, and possible *Hyaenodon* from both Ulangochuian and Duchesnean also support the correlation (Lucas, 1992; Robinson et al., 2004). *Brachyhyops neimongolensis* from the Ug₁ of the Erlian Basin is older than *B. trofimovi* and *B. viensis* from the late Eocene of Mongolia and North America, respectively, but shares similar size and morphologies with *B. wyomingensis* from the Duchesnean of North America (Wang and Qiu, 2002; Tsubamoto et al., 2011). Based on the preliminary paleomagnetic analyses, Wang et al. (2019) correlated the Ulangochuian Stage through chron C18.2n to C17, which can be roughly correlated to mostly Duchesnean and early Chadronian (Speijer et al., 2020).

CONCLUSIONS

The “East Mesa” is a pivotal area in the Shara Murun area, because it is intermediately located between the Baron Sog Mesa on the west and Erden Obo on the east, which are widely separated and difficult to correlate. Here we provide detailed litho- and biostratigraphy at the Bayan Obo, which is composed of possible Tukhum, Shara Murun, Ulan Gochu, and Baron Sog formations with about 70 m in thickness, and describe new materials of *Eomoropus major* and *Brachyhyops neimongolensis*. It is also the first report of *Eomoropus* from the Erlian Basin. We also provide detailed litho- and biostratigraphy at the Jhama Obo, which is composed of partial Shara Murun, Ulan Gochu, and Baron Sog formations with a total of about 50 m in thickness. Based on our recent fieldwork and CAE collection records, the correlation and faunal compositions of different sections in East Mesa is clarified, although the distribution of a few taxa conflict with previous viewpoints. Furthermore, the Ulangochuian ALMA is subdivided into Ug₁ and Ug₂, representing the faunas from the upper member of the Shara Murun Formation and the Ulan Gochu Formation, respectively. The Ulangochuian ALMA can be correlated to the Duchesnean NALMA based on the first appearances of *Amyndontopsis*, *Ardynomys*, *Brachyhyops*, and possibly *Hyaenodon* from both continents.

ACKNOWLEDGMENTS

We appreciate the discussion with Zhao-Qun Zhang (IVPP). We thank Wei Zhou, Shi-Jie Li, Qi Li, Yong-Xing Wang, and Yong-Fu Wang for assistance in the field; Wei Gao (IVPP) for the photography of the specimens; Yi-Han Yang (IVPP) for providing photos of figure panels 7A and B; and S. Bell, T. Baione, A. Gishlick, and J. Galkin (all AMNH) for providing literature access and assistance at the AMNH. We thank L. Holbrook and M. Muhlbachler for helpful comments and detailed editing of our English writing. We thank editors R. Voss and M. Knight (both AMNH) for the editorial comments. Funding was provided by grants from the National

Key Research and Development Project of China (grant no. 2024YFF0807603), National Natural Science Foundation of China (grant nos. 42272011, 42072023, and 41672014), Science & Technology Fundamental Resources Investigation Program (grant no. 2023YF100905), and Frick funds from the Division of Paleontology, American Museum of Natural History.

REFERENCES

- Bai, B. 2008. A review on Chinese Eocene chalicotheres *Eomoropus* and *Grangeria*. Proceedings of the 11th Annual Meeting of the Chinese Society of Vertebrate Paleontology: 19–30. Beijing: Ocean Press.
- Bai, B., and T. Qi. 2022. *Ulanodon*, a new name for the Hyracodontid *Ulania* Qi, 1990 (Perissodactyla, Mammalia). *Vertebrata Palasiatica* 60 (4): 328–329.
- Bai, B., Y.Q. Wang, and J. Meng. 2010. New craniodental materials of *Litolophus gobiensis* (Perissodactyla, “Eomoropidae”) from Inner Mongolia, China, and phylogenetic analyses of Eocene chalicotheres. *American Museum Novitates* 3688: 1–27.
- Bai, B., et al. 2018. Biostratigraphy and diversity of Paleogene perissodactyls from the Erlian Basin of Inner Mongolia, China. *American Museum Novitates* 3914: 1–60.
- Bai, B., J. Meng, C.M. Janis, Z.Q. Zhang, and Y.Q. Wang. 2020. Perissodactyl diversities and responses to climate changes as reflected by dental homogeneity during the Cenozoic in Asia. *Ecology and Evolution* 10 (13): 6333–6355.
- Bastl, K., and D. Nagel. 2014. First evidence of the tooth eruption sequence of the upper jaw in *Hyaenodon* (Hyaenodontidae, Mammalia) and new information on the ontogenetic development of its dentition. *Paläontologische Zeitschrift* 88 (4): 481–494.
- Bastl, K., D. Nagel, and S. Peigné. 2014. Milk tooth morphology of small-sized *Hyaenodon* (Hyaenodontidae, Mammalia) from the European Oligocene—evidence of a *Hyaenodon* lineage in Europe. *Palaeontographica Abteilung A* 303: 61–84.
- Berkey, C.P., and F.K. Morris. 1927. *Geology of Mongolia—a reconnaissance report based on the investigations of the years 1922–1923*, New York: American Museum of Nature History.
- Berkey, C.P., W. Granger, and F.K. Morris. 1929. Additional new formations in the later sediments of Mongolia. *American Museum Novitates* 385: 1–12.
- Burke, J.J. 1941. New fossil Leporidae from Mongolia. *American Museum Novitates* 1117: 1–23.
- Colbert, E.H. 1934. Chalicotheres from Mongolia and China in the American Museum. *Bulletin of American Museum of Natural History* 67 (8): 353–387.
- Colbert, E.H. 1938. *Brachyhyops*, a new bunodont artiodactyl from Beaver Divide, Wyoming. *Annals of the Carnegie Museum* 27: 87–108.
- Coombs, M.C. 1976. The taxonomic position of the chalicotheriid perissodactyl *Kyzylkakhippus orlovi* from the Oligocene of Kazakhstan. *Palaeontology* 19: 191–198.
- Dawson, M.R. 1968. Oligocene rodents (Mammalia) from East Mesa, Inner Mongolia. *American Museum Novitates* 2324: 1–12.
- Gaudin, T.J., R.J. Emry, and B. Pogue. 2006. A new genus and species of pangolin (Mammalia, Pholidota) from the late Eocene of Inner Mongolia, China. *Journal of Vertebrate Paleontology* 26 (1): 146–159.
- Gazin, C.L. 1956. The geology and vertebrate paleontology of upper Eocene strata in the northeastern part of the Wind River Basin, Wyoming. Part 2. The mammalian fauna of the Badwater Area. *Smithsonian Miscellaneous Collection* 131 (8): 1–35.

- Gilmore, C.W. 1931. Fossil turtles of Mongolia. *Bulletin of the American Museum of Natural History* 59 (4): 213–257.
- Gilmore, C.W. 1943. Fossil lizards of Mongolia. *Bulletin of the American Museum of Natural History* 81 (4): 361–384.
- Granger, W. 1928. [Records of fossils collected in Mongolia.] *Central Asiatic Expeditions. Field books of the Third Asiatic Expedition.* Archived at the American Museum of Natural History Library: 79 pp.
- Granger, W., and W.K. Gregory. 1943. A revision of the Mongolian titanotheres. *Bulletin of American Museum of Natural History* 80 (10): 349–389.
- Granger, W., W.K. Gregory, and H.F. Osborn. 1936. Further notes on the gigantic extinct rhinoceros, *Baluchitherium*, from the Oligocene of Mongolia. *Bulletin of the American Museum of Natural History* 72 (1): 1–73.
- Hu, C.K. 1959. Some Tertiary chalicotheres of northern China. *Vertebrata Palasiatica* 1 (3): 125–132.
- Li, C.K., and S.Y. Ting. 1983. The Paleogene mammals of China. *Bulletin of Carnegie Museum of Natural History* 21: 1–93.
- Li, Q. 2018. Additional cricetid and dipodid rodent material from the Erden Obo section, Erlian Basin (Nei Mongol, China) and its biochronological implications. *Palaeoworld* 27 (4): 490–505.
- Li, Q. 2024. New glires materials from the East Mesa, Erlian Basin (Nei Mongol, China). *Anatomical Record*: 1–12.
- Li, Q., and Q. Li. 2023. The Sharamurunian rodent fauna in the Erlian Basin, Nei Mongol, China. *Vertebrata Palasiatica* 61 (1): 43–70.
- Li, Q., Q. Li, R.C. Xu, and Y.Q. Wang. 2022. Rodent faunas, their paleogeographic pattern, and responses to climate changes from the early Eocene to the early Oligocene in Asia. *Frontiers in Ecology and Evolution* 10: 955779: 1–17.
- López-Torres, S., et al. 2023. Cranial endocast of *Anagale gobiensis* (Anagalidae) and its implications for early brain evolution in Euarchontoglires. *Palaeontology* 66 (3): 1–24.
- Lucas, S., S.G. Foss, and M. Muhlbachler. 2004. *Achaenodon* (Mammalia, Artiodactyla) from the Eocene Clarno Formation, Oregon, and the age of the Hancock Quarry Local fauna. In S.G. Lucas, K.E. Zeigler, and P.E. Kondrashov (editors), *Paleogene mammals.* New Mexico Museum of Natural History and Science Bulletin: 89–95.
- Lucas, S.G. 1992. Redefinition of the Duchesnean Land Mammal “Age,” late Eocene of western North America. In D.R. Prothero and W.A. Berggren (editors), *Eocene-Oligocene Climatic and Biotic Evolution*: 88–105. Princeton, NJ: Princeton University Press.
- Lucas, S.G., and R.M. Schoch. 1989. Taxonomy and biochronology of *Eomoropus* and *Grangeria*, Eocene chalicotheres from the western United States and China. In D.R. Prothero and R.M. Schoch (editors), *The evolution of perissodactyls*: 422–437. Oxford: Clarendon Press.
- Lucas, S.G., R.M. Schoch, and E. Manning. 1981. The systematics of *Forstercooperia*, a middle to late Eocene hyracodontid (Perissodactyla, Rhinocerotoida) from Asia and western North America. *Journal of Paleontology* 55 (4): 826–841.
- Meng, J., Y.M. Hu, and C.K. Li. 2005. *Gobiolagus* (Lagomorpha, Mammalia) from Eocene Ula Usu, Inner Mongolia, and comments on Eocene Lagomorphs of Asia. *Palaeontologia Electronica* 8 (1): 1–23.
- Meng, J., et al. 2007. New stratigraphic data from the Erlian Basin: Implications for the division, correlation, and definition of Paleogene lithological units in Nei Mongol (Inner Mongolia). *American Museum Novitates* 3570: 1–31.

- Mihlbachler, M.C. 2008. Species taxonomy, phylogeny, and biogeography of the Brontotheriidae (Mammalia: Perissodactyla). *Bulletin of the American Museum of Natural History* 311: 1–475.
- Osborn, H.F. 1929. *Embolotherium*, gen. nov., of the Ulan Gochu, Mongolia. *American Museum Novitates* 353: 1–20.
- Qiu, Z.X., and B.Y. Wang. 2007. Paraceratheres fossils of China. *Palaeontologia Sinica (new series C)* 29: 1–396.
- Radinsky, L.B. 1964a. Notes on Eocene and Oligocene fossil localities in Inner Mongolia. *American Museum Novitates* 2180: 1–11.
- Radinsky, L.B. 1964b. *Paleomoropus*, a new early Eocene chalicothere (Mammalia, Perissodactyla), and a revision of Eocene chalicotheres. *American Museum Novitates* 2179: 1–28.
- Radinsky, L.B. 1965. Early Tertiary Tapiroidea of Asia. *Bulletin of American Museum of Natural History* 129 (2): 181–264.
- Remy, J.A., et al. 2005. A new Chalicothere from the Pondaung Formation (late Middle Eocene of Myanmar). *Comptes Rendus Palevol* 4 (4): 341–349.
- Robinson, P., et al. 2004. Wasatchian through Duchesnean biochronology. In M.O. Woodburne (editor), *Late Cretaceous and Cenozoic mammals of North America*: 106–155. New York: Columbia University Press.
- Romer, A.S. 1966. *Vertebrate paleontology*. Chicago: University of Chicago Press.
- Simpson, G.G. 1931. A new insectivore from the Oligocene, Ulan Gochu horizon, of Mongolia. *American Museum Novitates* 505: 1–22.
- Speijer, R.P., H. Pälke, C.J. Hollis, J.J. Hooker, and J.G. Ogg. 2020. The Paleogene Period. In F.M. Gradstein, J.G. Ogg, M.D. Schmitz, and G.M. Ogg (editors), *Geologic Time Scale 2020*: 1087–1140. Amsterdam: Elsevier.
- Stock, C. 1933. An amynodont skull from the Sespe deposits, California. *Proceedings of the National Academy of Sciences of the United States of America* 19: 762–767.
- Storer, J.E. 1984. Fossil mammals of the Southfork Local Fauna (early Chadronian) of Saskatchewan. *Canadian Journal of Earth Sciences* 21 (12): 1400–1405.
- Sun, B., et al. 2009. Magnetostratigraphy of the Early Paleogene in the Erlian Basin. *Journal of Stratigraphy* 33: 62–68.
- Szalay, F.S., and S.J. Gould. 1966. Asiatic Mesonychidae (Mammalia, Condylarthra). *Bulletin of the American Museum of Natural History* 132 (2): 129–173.
- Szalay, F.S., and M.C. McKenna. 1971. Beginning of the age of mammals in Asia: the late Paleocene Gashato fauna, Mongolia. *Bulletin of the American Museum of Natural History* 144 (4): 271–317.
- Tong, Y.S., S.H. Zheng, and Z.D. Qiu. 1995. Cenozoic mammal ages of China. *Vertebrata Palasiatica* 33 (4): 290–314.
- Tsubamoto, T., M. Saneyoshi, M. Watabe, K. Tsogetbaatar, and B. Mainbayar. 2011. The entelodontid artiodactyl fauna from the Eocene Ergilin Dzo Formation of Mongolia with comments on *Brachyhyps* and the Khoer Dzan locality. *Paleontological Research* 15 (4): 258–268.
- Wall, W.P. 1981. Systematics, phylogeny, and functional morphology of the Amynodontidae (Perissodactyla: Rhinoceroidea). Ph.D. dissertation, Zoology Department, University of Massachusetts, Amherst.
- Wang, B.Y. 1997. Problems and recent advances in the division of the continental Oligocene. *Journal of Stratigraphy* 21 (2): 81–90.
- Wang, B.Y. 2007. Late Eocene lagomorphs from Nei Mongol, China. *Vertebrata Palasiatica* 45 (1): 43–58.

- Wang, B.Y. 2008. First Record of Late Eocene insectivores and chiropteres from Nei Mongol, China. *Vertebrata PalAsiatica* 46 (4): 249–264.
- Wang, B.Y., and J. Meng. 2009. *Ardynomys* (Cylindrodontidae, Rodentia) From Nei Mongol, China. *Vertebrata PalAsiatica* 47 (3): 240–244.
- Wang, B.Y., and Z.X. Qiu. 2002. A new species of Entelodontidae (Artiodactyla, Mammalia) from late Eocene of Nei Mongol, China. *Vertebrata PalAsiatica* 40 (3): 194–202.
- Wang, X.-Y., et al. 2020. A new species of *Amynodontopsis* (Perissodactyla: Amynodontidae) from the Middle Eocene of Jiyuan, Henan, China. *Vertebrata PalAsiatica* 58 (3): 188–203.
- Wang, Y.Q., et al. 2010. Early Paleogene stratigraphic sequences, mammalian evolution and its response to environmental changes in Erlian Basin, Inner Mongolia, China. *Science China Earth Sciences* 53 (12): 1918–1926.
- Wang, Y.Q., J. Meng, and X. Jin. 2012. Comments on Paleogene localities and stratigraphy in the Erlian Basin, Nei Mongol, China. *Vertebrata PalAsiatica* 50 (3): 181–203.
- Wang, Y.Q., et al. 2019. Paleogene integrative stratigraphy and timescale of China. *Science China Earth Sciences* 62 (1): 287–309.
- Wilson, J.A. 1971. Early Tertiary vertebrate faunas, Vieja Group, Trans-Pecos Texas: Entelodontidae. *Pearce-Sellards Series* 17: 1–17.
- Zdansky, O. 1930. Die alttertiären Säugetiere Chinas nebst stratigraphischen Bemerkungen. *Palaeontologia Sinica* (series C) 6 (2): 1–87.
- Zhang, Z.Q., et al., 2023. Cetacea and Artiodactyla I: Cetacea Artiodactyla I. *In* Z.X. Qiu and C.K. Li (editors), Basal synapsids and mammals. *Palaeovertebrata Sinica* 3, fascicle 9 (I) (serial no. 22-1): 1–263. Beijing: Science Press.

APPENDIX 1

FIELD RECORDS OF PALEOGENE FOSSILS BY THE GRANGER EXPEDITION IN 1928 FROM THE EAST MESA, ERLIAN BASIN, INNER MONGOLIA
 Asterisk indicates holotype; double dagger (‡), label identification.

Locality	Beds	Field no.	Field identification	AMNH no.	Published identification	Reference
Twin Oboes	From surface, just below Ulan Gochu	664	Lagomorph-miscell. jaws	26097, 26099, 26078, 26080-83	<i>Gobiolagus andrewsi</i> (26097), <i>Desmatolagus vetustus</i> (26099, 26080-26083)	Burke, 1941; Meng et al., 2005
	From surface, just below Ulan Gochu	666	?Bunodont artiodactyl, three jaw fragments, two individuals	26264, 99666	<i>Brachyhyops neimongolensis</i> *	Wang and Qiu, 2002
	Shara Murun beds	667	Creodont, lower jaw and fragment of maxilla	26065	<i>Mongolestes hadrodens</i>	Szalay and McKenna, 1971
	Shara Murun beds	667A	Lizard, back of skull and part of skeleton	6706	<i>Arretosaurus ornatus</i> *	Gilmore, 1943
	Mostly from Shara Murun beds	668	Miscellaneous: jaw fragments, foot bones, etc.	26263, 99670, 99671, 26750	<i>Lophiomeryx angarae</i> (26263), <i>Brachyhyops neimongolensis</i> (99670-99671), <i>Juxia sharamurensis</i> (26750)	Wang and Qiu, 2002; Qiu and Wang, 2007
	Shara Murun beds	669	Small rhinoceros-lower jaw	26027	<i>Deperetella</i> cf. <i>D. cristata</i>	Radinsky, 1965
	Shara Murun beds	670	Small rhinoceros-lower jaw	26028	<i>Triplopus turgaiensis</i> ‡	label
	Base of Ulan Gochu beds	671	Serpent-series of vertebrae	6709	Squatmata‡	label
	?	672	Small creodont hind foot & other parts of skeleton	26140	<i>Cryptomanis gobiensis</i> *	Gaudin et al., 2006
Twin Oboes ?	In place near base of Ulan Gochu beds	673	<i>Titanotherium</i> (Loucks), front of skull with lower jaws, milk and permanent dentition	26040	<i>Embolotherium grangeri</i>	Granger and Gregory, 1943; Mihlbachler, 2008
Twin Oboes	Shara Murun beds	678	Rhinocerotid, lower jaw	26030	<i>Metanymodon</i> sp.‡	label
	Base of Ulan Gochu beds	679	Small tortoise, complete shell	6692	<i>Testudo nanus</i> *	Gilmore, 1931
	Base of Ulan Gochu beds	680	Small tortoise, complete shell	6693	<i>Sharenys hemispherica</i>	Gilmore, 1931
	Base of Ulan Gochu beds	681	Small tortoise, complete shell	6694	<i>Sharenys hemispherica</i> *	Gilmore, 1931
	Ulan Gochu (not Shara Murun beds)	682	Titanotherid, lower jaws with dentition of one side	26012	<i>Titanodectes minor</i>	Granger and Gregory, 1943; Mihlbachler, 2008; Bai et al., 2018

APPENDIX 1 continued

Locality	Beds	Field no.	Field identification	AMNH no.	Published identification	Reference
	Basse of upper red beds, Ulan Gochu	727	Small carnivore or insectivore, skull, jaws and portions of skeleton	26079	<i>Anagale gobiensis</i> *	Simpson, 1931; López-Torres et al., 2023
	Base of Ulan Gochu beds	728	Lizard, jaw fragments of two or more individuals	6708, 6716	<i>Arretosaurus ornatus</i>	Gilmore, 1943
	Ulan Gochu beds			26097	<i>Gobiolagus andrewsi</i>	Meng et al., 2005
Jhama Obo	Ulan Gochu	662A	Perissodactyl fore foot	26264	<i>Brachyhyops</i> sp.‡	label
	Upper red beds (Ulan Gochu), found in place	662	Hyaenodont, pair of lower jaws	26066	<i>Hyaenodon pervagus</i>	Bastl et al., 2014
	Probably from Baron Sog beds, found on surface	663	Large rhinocerid, lower jaw fragment			
	Ulan Gochu beds	665	Miscellaneous: mostly artiodactyls, mostly jaw fragments	26016, 26017	<i>Didymoconus</i> sp. (26016),‡ <i>Desmatolagus vetustus</i> (26017)	label
	Ulan Gochu beds	674	Carnivores, rodents, etc., numerous jaws, skull, and fragments	26085, 26058–26060, 26086–26088, 26100, 26076–26077	<i>Hulgana ertinia</i> * <i>Ardynomyus</i> sp. (26076–26077)	Dawson, 1968; Wang and Meng, 2009
	Ulan Gochu beds	675	Turtle, fragments of shell and leg armor, two or more individuals	6696	<i>Testudo</i> sp.‡	label
	Ulan Gochu beds	676	Turtle, skull	6695	<i>Testudo</i> sp.	Gilmore, 1931
	Ulan Gochu (not Shara Murun beds)	677	Rhinocerid, left side of skull and lower jaws	26029	<i>Cadurcodon matthewi</i> *	Wall, 1981; Bai et al., 2018
	Baron Sog beds	686	<i>Baluchitherium</i> , miscell. foot and limb bones, etc.	26190, 26191	<i>Urtinotherium parvum</i> (26190)	Granger et al., 1936; Qiu and Wang, 2007
	Ulan Gochu (not Shara Murun) beds	687	<i>Titanotherium</i> , 7 vertebrae			
	Ulan Gochu (not Shara Murun beds)	688	Titanothere (Loucksi), skull	26010	<i>Embolotherium andrewsi</i>	Granger and Gregory, 1943; Mihlbachler, 2008; Bai et al., 2018
	Ulan Gochu (not Shara Murun) beds (near top)	689	Titanothere, lower jaws (young)	26013	<i>Titanotherium</i> sp.‡	label

APPENDIX 1 continued

Locality	Beds	Field no.	Field identification	AMNH no.	Published identification	Reference
South of Jhama Obo	Ulan Gochu (not Shara Murun) beds	700	Carnivore, lower jaw, fragments upper jaw	26064	<i>Mongolestes hadrodens</i> *	Szalay and Gould, 1966
	Ulan Gochu (not Shara Murun) beds	701	Titanotherid, skull front part right	26014	<i>Nasamplus progressus</i> *	Mihlbachler, 2008
	Ulan Gochu (not Shara Murun) beds	702	Rhinocerotid, lower jaw	26032	<i>Urtinotherium intermedium</i>	Qiu and Wang, 2007; Bai et al., 2018
	Ulan Gochu (not Shara Murun) beds	703	Rhinocerotid, lower jaws	26033	Metamynodontini‡	label
	Ulan Gochu (not Shara Murun) beds	704	Titanotherid, lower jaws (very large)	26005	<i>Titanodectes ingens</i> *	Granger and Gregory, 1943; Mihlbachler, 2008; Bai et al., 2018
	Ulan Gochu (not Shara Murun) beds	705	Carnivore	26067	<i>Hyaenodon</i> sp.	Bastl and Nagel, 2014
	Base of Ulan Gochu beds	706	Titanotherid, foot fragment	?		
	Ulan Gochu (not Shara Murun) beds	707	Titanotherid, lower jaw m1-3	26105	<i>Titanotherium</i> sp.‡	label
	Ulan Gochu beds	726	Rhinocerotid, front of skull and lower jaws, good teeth	26038	<i>Amynodontopsis parvidens</i>	Wall, 1981; Bai et al., 2018
	Ulan Gochu beds			26091, 26092	<i>Gobiolagus andrewsi</i> *	Meng et al., 2005
			26089	<i>Desmatolagus vetustus</i> *	Meng et al., 2005	
Ulan Shireh Obo	Base of Ulan Gochu beds	683	Titanotherid (Loucksi), skull and lower jaws	26009	<i>Embolotherium andrewsi</i>	Granger and Gregory, 1943; Mihlbachler, 2008; Bai et al., 2018
	Ulan Gochu (not Shara Murun) beds	684	Rhinocerotid, lower jaws	26031	<i>Amynodontopsis tholoz</i>	Wall, 1981; Bai et al., 2018
	Possibly Baron Sog	685	Small rhinocerotid, skull with much worn teeth	26178	<i>Amynodontopsis parvidens</i>	Wall, 1981; Bai et al., 2018
Ulan Shireh Obo	Top of gray Ulan Gochu (not Shara Murun) beds, channel deposit	708	Titanotherid (Loucksi), fine skull with complete nasals	26000	<i>Embolotherium andrewsi</i>	Granger and Gregory, 1943; Mihlbachler, 2008; Bai et al., 2018
	Top of gray Ulan Gochu (not Shara Murun) beds, channel deposit	709	Rhinocerotid, skull and jaws	26035	<i>Amynodontopsis tholoz</i> *	Wall, 1981; Bai et al., 2018

APPENDIX 1 continued

Locality	Beds	Field no.	Field identification	AMNH no.	Published identification	Reference
	Top of gray Ulan Gochu (not Shara Murun) beds	710	Rhinocerotid, skull	26034	<i>Zaisanamyndon borisovi</i>	Wall, 1981; Bai et al., 2018
	Ulan Gochu (not Shara Murun beds)	711	Small rhinocerotid, lower jaw	26036	<i>Juxia sharamurenensis</i> †	label
Spring Camp	Shara Murun beds	715	Miscellanea teeth, foot bones, etc. ?			
	Shara Murun beds	716	Titanotherid, anterior part of lower jaw	26132	<i>Titanodectes minor</i> *	Granger and Gregory, 1943; Mihlbachler, 2008; Bai et al., 2018
	Shara Murun beds	717	Titanotherid, lower jaws	26131	<i>Parabrontops</i> cf. <i>P. gobiensis</i>	Granger and Gregory, 1943; Mihlbachler, 2008; Bai et al., 2018
	Shara Murun beds	718	Hyaenodont, lower jaws	26137	<i>Pterodon hyaenoides</i> †	label
	Shara Murun beds	719	Rhinocerotid, anterior part of a lower jaw	26133	<i>Sharamyndon mongoliensis</i> †	label
	Lower red beds (?Arshanto)	720	Titanotherid, skull, top weathered off	26104	<i>Protitan grangeri</i> (= <i>P. bellus</i> *)	Granger and Gregory, 1943; Mihlbachler, 2008; Bai et al., 2018
	Shara Murun beds	721	Rhinoceros, one side of skull	26136	Amyodontidae†	label
	Shara Murun beds	722	Rhinocerotid, lower cheek teeth	26134	Amyodontidae†	label
6 mi E of Spring Camp	?Shara Murun beds	723	Rhinocerotid	26037	<i>Juxia sharamurenensis</i> †	label
Spring Camp	Shara Murun beds	724	Large lophodont, lower jaws	26056	<i>Pappaceras minuta</i>	Lucas et al., 1981; Bai et al., 2018
	Shara Murun beds	725	Rhinocerotid, lower jaw	26135	<i>Cadurcodon ardyensis</i> †	label